Limnological, Sediment, and Aquatic Macrophyte Biomass Characteristics in Half Moon Lake, Eau Claire, Wisconsin, 2016

Interim Letter Report
29 December, 2016

William F. James
University of Wisconsin – Stout
Sustainability Sciences Institute Discovery Center – 123 E Jarvis Hall
Center for Limnological Research and Rehabilitation
Menomonie, Wisconsin 54751

BACKGROUND AND OBJECTIVES

Management to reduce internal phosphorus (P) loading and algal growth to improve underwater light condition for native aquatic plants has been threefold for Half Moon Lake, Eau Claire, Wisconsin (James et al. 2002). Motor boat activity has been restricted on the lake to reduce P resuspension. Canopy-shading of native macrophytes and P recycling caused by curly-leaf pondweed decomposition were controlled by annual early spring herbicide treatments during the years 2009-2014 and 2016 to selectively target this species with minimal impact to native plants. Finally, P release from sediments was managed during the year 2011 (application occurred during 15-18 June, 2011) using buffered alum-aluminate to drive algal productivity toward P-limited growth. The goal was to decrease internal P loading from sediment by at least 90% in order to reduce algal biomass and increase light penetration. The objectives of this interim letter report are to describe limnological conditions and aquatic macrophyte response in 2016 to overall lake rehabilitation.

METHODS

Lake Limnological Monitoring

Six stations were established in the lake for water quality monitoring purposes (Figure 1; Table 1). Monitoring was conducted biweekly at each station between May and early October, 2016. Water temperature, dissolved oxygen, conductivity, and pH were measured in situ at 0.5-m intervals using a sonde unit (Hydrolab Quanta, Hach Inc., Loveland, CO) that was precalibrated against known standards and Winkler titrations. Secchi disk transparency was measured at each station by lowering a 20-cm diameter alternating black and white disk into the water column until it could not be seen, then slowly pulling it back up until visible, and recording the depth of visibility. Underwater photosynthetically-active radiation (PAR) was measured at 25-cm intervals using a cosine quantum radiometer (Model LI1000, Li-Cor, Inc., Lincoln, NE). The light attenuation coefficient was calculated as,

$$k_d = \frac{\ln(I_o) - \ln(I_z)}{z}$$

where I_o is the surface PAR ($\mu E/cm^2$ s) and I_z is the PAR at depth z (m). In general, k_d is inversely related to Secchi disk transparency. Thus, higher k_d reflects lower light penetration into the water column and a lower Secchi disk transparency.

Water samples integrated over the upper 1 m were collected biweekly for analysis of total P, soluble reactive P, and viable chlorophyll. Total P samples were predigested with potassium persulfate according to Ameel et al. (1993). Total and soluble reactive P (i.e., P available for uptake by algae) were analyzed colorimetrically using the ascorbic acid method (APHA 2005). Samples for viable chlorophyll (i.e., a surrogate measure of algal biomass) were filtered onto glass fiber filters (Gelman A/E; 2.0 µ nominal pore size) and extracted in 50:50 dimethyl sulfoxide:acetone before fluorometric determination (Welchmeyer 1994).

Storm Sewer Monitoring

Automated storm water samplers (ISCO model 6700) and flow loggers equipped with area-velocity sensors (ISCO model 4150) were deployed at 3 storm sewers in 2016 to determine phosphorus concentration and loading (Figure 1). Vandalism resulted in destruction of the sampling station at storm sewer 3 in 2014 (Figure 1). Vandalism of station 2 in 2016 resulted in a data gap. Loggers were programmed to monitor stage and velocity at 5-min intervals. Storm water samplers collected discrete samples at 15-min intervals during precipitation and runoff events. The discrete samples were composited via flow-weighting in the laboratory for determination of total and soluble reactive P.

Sediment Chemistry

Sediment cores were collected at station 10 and 30 in late June, 2016, for determination of sediment P fractions and rates of P release under anaerobic conditions. A core from each station was sectioned at 1- to 2.5-cm intervals for determination of loosely-bound, iron-bound, and aluminum-bound P using methods described in Hieltjes and Lijklema (1980), Psenner and Puckso (1988), and Nürnberg (1988). Additional subsamples were dried at 105 °C to a constant weight and burned at 500 ^{o}C for determination of moisture content, sediment wet and dry bulk density, and organic matter content (Håkanson and Jansson 2002).

Five replicate cores were also collected at each station for determination of P release from sediment under anaerobic conditions. The cores were drained of overlying water and the upper 10 cm of sediment was transferred intact to a smaller acrylic core liner (6.5-cm dia and 20-cm ht) using a core remover tool. Surface water collected from the lake was filtered through a glass fiber filter (Gelman A-E) and 300 mL was siphoned onto the sediment contained in the small acrylic core liner without causing sediment resuspension. Sediment incubation systems were placed in the darkened environmental chamber and incubated at a constant temperature (20 ^{o}C). The oxidation-reduction environment in the overlying water was controlled by gently bubbling nitrogen (anaerobic) through an air stone placed just above the sediment surface in each system.

Water samples for soluble reactive P were collected from the center of each system using an acid-washed syringe and filtered through a 0.45 µm membrane syringe filter (Nalge). The water volume removed from each system during sampling was replaced by addition of filtered lake water preadjusted to the proper oxidation-reduction condition. These volumes were accurately measured for determination of dilution effects. Soluble reactive P was measured colorimetrically using the ascorbic acid method (APHA 2005). Rates of P release from the sediment (mg/m^2 d) were calculated as the linear change in mass in the overlying water divided by time (days) and the area (m^2) of the incubation

core liner. Regression analysis was used to estimate rates over the linear portion of the data.

Aquatic Macrophytes

In June and August, 2016, submersed macrophyte biomass was quantified at ~150 stations in the lake using the point-intercept method (Madsen, 1993). In early May, numbers of germinated curly-leaf pondweed turions per square meter were quantified at each station. A rake-pull method was used to collect samples. The rake was lowered to the sediment and raised to the lake surface at a constant, slow rate while twisting the handle to snag macrophyte stems within a ~ 0.13 m^2 area. The samples were sorted by species and dried to a constant mass at 65 ^oC in a forced-air drying oven. Biomass (g/m^2) at each station was estimated as dry mass divided by the circular area covered by a 180 degree twist of the rake. The rake-pull method provides a reasonably accurate biomass estimate for species such as curly-leaf pondweed and Eurasian watermilfoil that is comparable to diver quadrat sampling (Johnson 2010). However, it overestimates biomass in areas dominated by coontail, elodea, and flat-stemmed pondweed because these species tend to inter-tangle with plants outside the quadrat area, resulting in unintended sampling from an area wider than that of the rake diameter (Johnson 2010). Thus, caution needs to be used when interpreting biomass data dominated by these species.

RESULTS AND DISCUSSION

Sediment characteristics in 201

Al treatment occurred during the period 15-18 June, 2011. The target dosage goal for the western arm of the lake was 150 g Al/m^2 while the eastern arm and southern (i.e., south of the causeway) embayment target concentration was 75 g Al/m^2. Braun's Bay was not treated with Al.

In 2016, detailed inspection of sediment moisture content and wet bulk density vertical profile characteristics suggested that the Al floc was still largely positioned on top of the original sediment interface. For cores collected in the western arm of the lake (i.e., station 10) in 2016, sediment wet bulk density was very low, while moisture content approached 95%, in the upper 3- to 4-cm layer, contrasting substantially with original surface sediment physical characteristics before the Al treatment (Figure 2). East arm sediments exhibited a similar pattern of lower wet bulk density and higher moisture content over the upper 1-cm layer compared to 2010 conditions (Figure 3). Differences in the apparent thickness of these layers were probably attributed to application of 2X more Al (i.e., 150 g/m^2) in the west versus the east (i.e., 75 g/m^2) arm of the lake.

Trends in surface physical-textural sediment characteristics indicated that the Al floc layer (upper ~3 cm for station 10 and 1 cm for station 30) has been consolidating 5 years post-treatment (Figure 4). For instance, empirically-derived wet bulk density and solids content have increased while moisture content has decreased over the 5-year period at both station locations. This pattern may be due to a couple of factors. The Al floc has been consolidating over time and some burial by new sediment deposits may be resulting in additional compaction. Overall, however, the Al floc appears to be largely overlaying the original sediment 5 years post-treatment. Higher moisture content and lower wet bulk density and solids content in the Al floc versus the original sediments 5 years post-treatment suggest that little mixing with the original sediment has occurred due to sediment density differences between the two layers. This is not surprising since Half Moon Lake is sheltered from wind-induced resuspension and exposure to wave orbitals.

Prior to Al treatment in 2010, iron-bound P concentrations were greatest in the upper 5-cm sediment layer at both stations. Concentrations within this layer were greatest in west arm, exceeding 1.5 mg/g (Figure 2), versus much lower iron-bound P concentrations in east arm sediments (0.32 mg/g; Figure 3). In 2016, iron-bound P concentrations in west arm sediments were relatively high in the upper 3 cm Al layer and increased substantially at depths below the original 2010 sediment interface, reflecting 2010

concentrations. In particular, iron-bound P concentrations now exceed 0.50 mg/g and 0.2 mg/g in the Al floc layer at stations 10 and 30, respectively (Figure 2 and 3).

Aluminum-bound P concentrations were maximal in the upper 2- to 3-cm Al floc layer situated above the original sediment surface in west and east arm sediments (Figure 2 and 3). Although 2016 Al concentration information was not available at the time of the interim report, vertical profiles collected in 2014 indicated that the Al floc was situated in the surface 2- to 3-cm (Figure 5), coinciding with peak aluminum-bound P concentrations observed in 2015. Measured Al concentrations of 132 g/m^2 in the west arm and 89 g/m^2 in the east arm sediments were close to target application concentrations of 150 and 75 g/m^2, respectively. The Al:P ratio in the Al floc was 33:1 and 55:1 for west and east arm areas, respectively, in 2014.

Annual trends in surface Al floc layer of redox-P suggested that concentrations are increasing over time since Al treatment (Figure 6). Redox-P in west arm sediments was very low in the Al floc layer shortly after treatment in 2011. Concentrations increased linearly between 2011 and 2014 and have leveled off in 2015 and 2016 to ~ 0.65 mg/g. This buildup over time and may be related to upward diffusion of porewater iron and P into the Al floc from sediments located below the original interface. Although much lower in concentration, redox-P has also increased in the Al floc layer at station 30 over time post Al treatment (Figure 6). Between-arm differences in redox-sensitive P concentrations in the Al floc layer in 2016 were probably related to concentration differences in the original sediment surface layer prior to Al application (Figure 6).

Aluminum-bound P increased over time in the Al floc layer at both stations between 2011 and 2014 and has either leveled off (as for station 10) or started to decline (as for station 30, Figure 6). For instance, concentrations have increased from ~ 1.4 mg/g in 2011, shortly after Al application, to greater than 2.0 mg/g in 2016 in the Al floc layer of station 10 sediments. Although lower in concentration, station 30 Al floc layer sediments increased in concentration from ~ 0.70 mg/g in 2011 to greater than 0.9 mg/g in 2015. Lower concentrations in 2016 may reflect deposition of new sediment and dilution of

aluminum-bound P. Overall, these patterns indicated that P binding onto $Al(OH)_3$ has been occurring.

Strong vertical P (and Fe) concentration gradients between original surface sediment and the overlying Al floc sediments may be driving upward P diffusion into the Al floc over time, as suggested by 2014 vertical sediment profiles (Figure 7). Both iron-bound and aluminum-bound P concentrations were elevated in the alum floc layer at both stations in 2014. This pattern suggested that while a substantial fraction of the total mobile P (i.e., the sum of iron-bound and aluminum-bound P) diffusing into the Al floc was sequestered by $Al(OH)_3$, some of this P was also apparently adsorbed by Fe and has now become a source of internal P loading to Half Moon Lake.

Incomplete or inefficient binding of total mobile P by $Al(OH)_3$ may be attributed to two factors. First, de Vicente et al. (2008a) found that P binding efficiency diminished rapidly and substantially as $Al(OH)_3$ aged and became a more ordered crystalline structure, particularly in the absence of initial exposure to PO_4 shortly after application. Aging and polymerization may lead to unfilled binding sites located in the interior crystalline structure and a longer molecular P diffusional path length that limits P binding efficiency. Thus, P binding rate efficiency may have become limited over time by diffusional path length to the crystalline interior. Second, strong vertical concentration gradients in the porewater below the Al floc would result in upward diffusional P and Fe (and other constituents) flux into the Al floc. If this vertical P diffusional rate exceeded the rate of molecular P diffusion into the crystalline interior of $Al(OH)_3$ polymers, binding of total mobile P could be incomplete, resulting in porewater P that can become readsorbed to Fe(OOH), enter redox-mediated recycling pathways, and once again become an internal P load to the lake. Thus, $Al(OH)_3$ polymerization coupled with high redox-P concentrations in the original surface sediment may be responsible for reduced P binding efficiency leading to reduced longevity and effectiveness in controlling internal P loading.

Changes in the areal redox-P, aluminum-bound P, and combined total mobile P concentration supported the above suggestions (Figure 8). For station 10 sediment, total mobile P concentrations have increased in the Al floc layer between 2011 and 2015. Aluminum-bound P has accounted for most of the areal total mobile P. However, areal concentrations of redox-P have also increased, suggesting incomplete P binding by the Al floc and, consequently, readsorption of diffused P to Fe and redox-mediated recycling. Total mobile P flux into the Al floc layer was greatest between 2011 and 2013 but has declined annually thereafter. In contrast, redox-P flux into the Al floc layer has slightly increased between 2013 and 2015. As a result, total P binding efficiency has declined from ~ 90% between 2011 and 2013, to ~ 70% between 2011 and 2015 (Figure 8). Annual P binding efficiency (i.e., between year-1 and year-2) between 2014 and 2015 declined to only ~ 55% (Figure 9). These results further suggest that P binding efficiency has declined and imply that upward P diffusion from deeper layers is overwhelming P binding efficiency in the Al floc.

Laboratory-derived rates of P release from sediment for west arm sediments under anaerobic conditions increased from undetectable during the first 2 years post-treatment to a mean 4.02 mg/m^2 d (± 0.92 SE; n = 5) by 2016 (Figure 10). While the 2016 anaerobic P release rate was a ~ 66% decrease from the pretreatment mean of 11.8 mg/m^2 d (±1.7 SE) it, nevertheless, represented a potential source of P to the water column. For east arm sediments, the anaerobic P release rate was essentially undetectable during the 2011-13 post-treatment years but has increased to a mean 1.18 mg/m^2 d (± 0.24 SE) in 2016 (Figure 10). Anoxic and hypoxic conditions were detected above the sediment interface at west arm stations 10 and 20 in July through August, 201 (Figure 11). East arm stations 30 and 40 exhibited bottom-water anoxia primarily in August, 2016 (Figure 12). Station 50 and 60 did not exhibit bottom water anoxia; however, concentration declined to less than 2 mg/L at station 50 in late August and at station 60 in early June (Figure 13).

Water quality trends after Al treatment

Total P and chlorophyll concentrations were lowest at west arm stations 10 and 20 in May and increased to a maximum by September (Figure 14 and 15). Peak total P concentrations in September exceeded 0.050 mg/L (range = 0.037 to 0.064 mg/L, Figure 14). Interestingly, chlorophyll concentrations were very moderate (generally less than 30 µg/L) between May and mid-July, but then increased to peaks between mid-August and September at these west arm stations (Figure 15). The mean chlorophyll concentration during this period was ~ 60 µg/L, and ranged between 40 and 84 µg/L. Secchi transparencies were high at west arm stations in May through early June, often down to the lake bottom (Figure 14). They declined in conjunction with moderate chlorophyll levels between mid-June and July, but exceeded 1 m (range = 1 to 2 m). Secchi transparencies declined below 1 m in conjunction with chlorophyll bloom initiation in mid-August and were ~ 0.7 m during peak chlorophyll in September (Figure 16). The light attenuation coefficient, k_d, increased to maxima near 3 m^{-1} at west arm stations during the September chlorophyll bloom, indicating severe PAR limitation for summer submersed macrophyte communities (Figure 17).

The eastern arm (stations 30 and 40) of the lake exhibited somewhat seasonally lower total P, chlorophyll, and k_d, and higher Secchi transparency, during the height of the phytoplankton growing season compared to the western arm (Figures 14-17). However, prominent peaks in chlorophyll approached or exceeded 60 µg/L by late August with concomitant decreases in Secchi transparency to less than 1 m. In contrast, south embayment (station 50) exhibited lower total P and chlorophyll concentrations compared to main arm stations. Secchi transparency exceeded 1 m between May and mid-July then declined to ~ 1 m from mid-August through September. PAR attenuation was greater than 2 in late September in conjunction with moderate chlorophyll concentration peaks.

Trends at station 60 (i.e., Braun's Bay) contrasted sharply from those observed in the main basin of the lake. We had difficulties with inadvertently hitting submersed aquatic macrophytes using the 1-m integrated sampler and contaminating water samples with

periphyton, so switched to surface sampling in August (Figures 14-17). Total P concentrations peaked in early June (Figure 14) but chlorophyll was very low while Secchi transparency exceeded the lake bottom (Figure 15 and 16). This total P pattern may have reflected zooplankton biomass during the clearing period. Otherwise, surface total P concentrations in August through September were usually less than 0.03 mg/L, surface chlorophyll concentrations were less than 10 µg/L. Secchi transparencies reached the lake bottom throughout the summer and k_d was very moderate to low, usually less than 1 m^{-1}.

Overall trends in July-September mean total P, chlorophyll, and Secchi transparency in the main basin (i.e., stations 10-40) are shown in Figure 18. The period July-September was chosen because it represented the typical period of maximum nuisance algal blooms and did not include the late May-June clearing phase caused by zooplankton grazing. Mean total P and chlorophyll were slightly lower, while Secchi transparency improved, in 2016 relative to 2015 (Table 2 and 3). However, the mean chlorophyll concentration for 2016 approached means observed in 2008 and 2010, before Al treatment. Trends in mean summer total P, chlorophyll, and Secchi transparency for various areas of the lake indicated that impairment was greatest in the west arm while south embayment variables reflected continued improved water quality conditions post-treatment (Figure 19). Mixing and water exchanges between the east and west arms may explain much of the mean summer total P and chlorophyll concentrations increase, and Secchi transparency decrease, in the east arm. Overall, trends in limnological response variables in the east and west arms coincided with trends of increasing laboratory-derived anaerobic diffusive P flux from west arm sediments.

Predicted maximum inhabitable depth for stem- and rosette-forming submersed macrophytes, based on the percentage of surface PAR radiation penetrating the water column and Secchi transparency (Middelboe and Markager 1997), continued to decline in 2016 (Figure 20). Underwater PAR habitat impairment was greatest in the west arm (Figure 21), which may be impacting native biomass in 2016 (see below). The predicted maximum inhabitable depth was 2.4 m for stem-forming submersed macrophytes and 1.0

m for rosette- and meadow-forming submersed macrophytes. The maximum colonizable depth was ~ 2.1 m for stem-forming macrophytes, equivalent to the water column depth, and 0.9 m for rosette-forming macrophytes in the south arm in 2016.

Trends in the percent improvement in limnological response variables over pretreatment values have declined to 50% or less in 2016 (Figure 22). Summer total P and chlorophyll means were 49% and 34%, respectively, in 2016 compared to the pretreatment means while Secchi transparency was only 16% deeper compared to the pretreatment mean. The 2016 improvement in the PAR attenuation coefficient and maximum inhabitable depth for stem- and rosette-forming macrophytes versus pretreatment conditions were 43%, 47%, and 43%, respectively.

Post herbicide treatment trends in curly-leaf pondweed and native submersed vegetation

Early spring endothall applications for selective control of curly-leaf pondweed (CLP) ended in 2014 after 5 consecutive years of treatment. Surprisingly, CLP growth rebounded after herbicide treatment cessation in spring 2014 and was present at over 40% of the point-intercept locations by June, 2014 (Figure 23). June, 2014, biomass also rebounded substantially from other treatment years to a lakewide average of 20 g/m^2 (Figure 23). By early April, 2015, germinated CLP turion frequency of occurrence increased substantially to greater than 60%, clearly indicating that the turion bank in the sediment was still viable after 5 consecutive years of control (Figure 24). A Second 5-year Endothall application program was initiated in April, 2015. CLP frequency of occurrence and biomass in June and August declined to near zero in response to the 2015 and 2016 application (Figure 23).

CLP germinated turion frequency of occurrence and numbers/m^2 were elevated in April, 2016, despite herbicide control in 2015 (Figure 24). The winter of 2015-16 was mild with little snow cover on the lake, promoting light penetration for winter germination and growth. Thus sampling in April, 2016, captured high germinated turion numbers

compared to other years. Previous results have indicated that substantial turion germination in Half Moon Lake can occur as late as May.

Native submersed macrophyte frequency of occurrence biomass was again dominated by Elodea in 2016; some other native species were also observed (Stargrass, wild celery, coontail). In addition, native frequency of occurrence and biomass rebounded slightly in 2016 from lower percentages in 2014-15 (Figure 25). Biomass declines were greatest in the deeper west arm of the lake (not shown). Overall annual trends in August native biomass suggest that it is very sensitive to Secchi transparency and k_d. There was a strong linear relationship between mean (July-September) Secchi transparency and August mean native biomass and a weaker negative linear relationship between PAR attenuation coefficient and August mean native biomass (Figure 26).

Storm sewer hydrology and phosphorus inputs to Half Moon Lake

During the summer period, monthly rainfall was above normal in June and September, 2016 (Figure 27). Storms exceeding 1 inch of rainfall occurred in late May, mid-June, early July, early August, and mid-September (Figure 28). Overall, precipitation in 2016 was above the ~20 inch average for the May-September period at ~ 26 inches.

Approximately 71 storm-related or base flow events were collectively captured at storm sewers 1, 2, and 4 for determination of total and soluble reactive P concentrations in 2016. Unfortunately, the equipment box located at storm sewer 3 was vandalized in 2014 and removed from the study. Flow increased at all monitored storm sewers as a result of storms (Figure 29-31). At storm sewer 1, shallow groundwater pumps (up to 3 pumps) provided a continuous base flow of Chippewa River groundwater to Half Moon Lake (Figure 29). Three pumps appeared to be operational during the study period, providing a base flow of ~ 2.58 ft^3/s (Figure 29).

Mean summer (i.e., June-September) storm flow at station 2 and 4 were also elevated in 2016 (Figure 30-31 and Table 4). Storm flow at station 1 in 2016 was within ranges

observed during other years. However, relationships between mean summer flow and precipitation were weak. This pattern may be due to variations in storm intensity and duration. For instance, a higher precipitation summer but with lower intensity might result in greater infiltration than a summer with lower precipitation but with greater intensity storms. Mean base flow at storm sewer 1 was relatively high in 2016 due to operation of three pumps throughout the summer. Measured mean storm flow was greatest at sewer 1 at 0.1196 ft^3/s, followed by sewer 2 at 0.0457 ft^3/s, and sewer 4 at 0.0196 ft^3/s (Figure 32 and Table 4).

The measured mean storm flow-weighted total P concentration was greatest for storm sewer 1 at 0.410 mg/L (Figure 33 and Table 5). This mean fell within ranges for other years. In contrast, the mean storm flow-weighted total P concentration was much lower in 2015 (Table 5). We had difficulty with trash wrapping around and blocking the sampling line in 2015. This issue often disrupted automated sampling, leading to frequent sampling errors. Attempts at repositioning the sampler intake did not correct the problem. In 2016, the sampler intake was positioned on the culvert bottom and secured with clamps, resulting in improved sampling.

Base-flow total P at storm sewer 1 was 0.085 mg/L, which was comparable to base-flow concentrations during other years (Table 5). Mean total P was moderately high at 0.121 and 0.170 mg/L for storm sewers 2 and 4, respectively, in 2016 and comparable to mean concentrations during other years. Mean storm flow soluble reactive P concentrations ranged between 0.015 mg/L (i.e., storm sewer 2) and 0.045- 0.058 mg/L (i.e., storm sewers 1 and 4).

As in previous years, storm sewer 1 dominated measured total and soluble reactive P loading in 2016 (Figure 34 and Tables 6 and 7). Base-flow from the Owen Park pumps provided the majority of the total P load to the lake (Table 6 and 7). Over the June-September summer period, storm sewer 1 discharged ~ 65 kg total P and 34 kg SRP. Storm sewer 1 base flow contributed most of the SRP loading, which represented 50% of the base flow total P loading. By comparison, SRP loading accounted for only 10% of the

storm flow total P load at this site. Storm sewer 2, which drained a much smaller subwatershed, contributed only ~1.6 kg total P over the summer period and SRP accounted for ~ 12% of this load. Storm sewer 4, which received drainage from the Carson Park stadium parking lot that discharges into Braun's Bay, contributed ~ 0.7 kg total P over the summer. SRP represented 34% of the total P load from this site.

MANAGEMENT RECOMMENDATIONS

Curly-leaf pondweed

It is apparent that the turion bank in Half Moon Lake sediments was still viable after 6 years of early spring endothall treatments. An additional 5-year early spring endothall treatment program was initated for 2015 through 2018. However, the number of treatment years required to reduce the turion bank remains unknown. Other studies have reported some CLP suppression after up to 7 years of herbicide control (Johnson et al 2012). Research findings on longer-term treatment programs have not been published. However, additional management via early spring endothall treatments may be required for several years.

Quantifying turion germination has become more problematic in light of recent findings. It appears that turion germination is very significant in April and May. Ideally, seasonal germination patterns should be examined in order to better understand and predict the optimal timing for treatment. A caveat has been that treatments have generally occurred in late April in conjunction with a water temperature range of 15 to 18 C to maximize selective control of CLP. While April point-intercept sampling has generally shown a declining germination trend over time, this approach has failed to account for projected later germination. Additionally, herbicide applications have probably inadvertently controlled these later germinations, as indicated by frequency and biomass trends in June. Germinated turion assessment will continue in later spring to more accurately quantify frequency of germinated turions. Ultimately, depletion of the turion

bank can best be assessed by evaluating frequency and biomass during a nontreatment year.

Algal blooms and PAR attenuation

The native macrophyte community is clearly being impacted by high PAR attenuation, particularly in the west arm of the lake, due to the reemergence of cyanobacterial blooms in 2014-2016. The current working hypothesis suggests that porewater Fe and P have slowly diffused from deeper sediment layers into the surface Al floc layer over time. While the Al floc is sequestering some of this P, another portion is now coupled with Fe and can diffuse into the overlying water column under reducing conditions. More importantly, this P is directly available for uptake by cyanobacterial spores residing in the sediment of Half Moon Lake (i.e., working hypothesis). Even though an adequate Al dosage was applied to inactivate the high sediment mobile P concentrations, the Al floc did not sink into the upper sediment due to higher bulk density characteristics of the original sediment interface. Thus, Al binding efficiency has decreased over time (de Vicente et al. 2008a and b), allowing for upward P diffusion through the Al floc and re-adsorption onto Fe~(OOH) (Lewendowski et al. 2003). This outcome is most apparent in west arm sediments, where mobile P concentrations were extraordinarily high in the original surface sediment layer. Although similar diffusional processes are occurring in east arm sediments, much less mobile P has accumulated in the surface Al floc layer due to lower mobile P concentrations in the original surface sediment layer.

Because mobile P concentrations were so high in the original sediment column and the Al floc could not sink into the sediment to sequester this P, upward P diffusion is likely to continue, reducing Al treatment success and longevity in Half Moon Lake. Thus, long-term Al management (i.e., over several years to decades) is required that involves applications every 2 to 5 years. Al dosage should target binding mobile P in the current Al floc layer (i.e., the upper 3 cm in the west arm and the upper 2 cm in the east arm). Because bulk densities are lower in these layers, addition of a new Al floc has a greater probability of sinking through these surface layers to bind mobile P. De Vicente et al.

(2008b) similarly suggested that smaller Al doses spread out over several years might maintain higher P binding efficiencies.

Al dose and application for 2017

Location of the Al floc on the sediment surface and diminished P binding efficiency due to crystallization need to be considered in the management of internal P loading in Half Moon Lake. Findings here indicated that the success and longevity of a single, large dose, application depended on adding enough Al to sequester and control internal P loading while compensating for Al polymerization and P binding inefficiency. This management scenario will be more expensive, inefficient, and shorter-lived.

Application of multiple lower Al concentrations spread out over a period of years will be more effective in filling binding sites, lowering the Al:P binding ratio, and stabilizing polymerization for longer internal P loading control and at a lower overall cost. For Half Moon Lake, an adaptive management approach of applying lower Al concentrations spread out over a period of years (i.e., 2-5 year intervals) and monitoring lake response for future Al maintenance applications will lead to greater longevity and more effective control of internal P loading. In contrast, the success and longevity of another large dose Al application depends on adding enough Al to sequester and control internal P loading while compensating for Al polymerization and P binding inefficiency. This management scenario will be more expensive and inefficient.

Since the Al application in the west arm sediments has lost 40% of its P binding effectiveness, an additional Al treatment is recommended in that area of the lake in 2017. An Al dose of ~ 50 g/m^2 within the 10-ft contour is expected to provide internal P loading control over a period of at least 2-3 years (Table 8). Both west and east arm sediment will continue to be monitored for P binding efficiency and internal P loading control annually as part of an adaptive management plan to support decisions regarding additional lower Al dose applications in the future. It is anticipated that lower dose Al applications on the order to ~25 g/m^2 in the east arm and 50 g/m^2 in the west arm at 2 to 5

year intervals will be needed over a period of 10 to 15 years to completely control internal P loading in the lake. This dosage and application scenario will be much more cost effective compared to another larger Al dose application as was conducted in 2011.

An example of an Al application scenario is shown in Table 9. Low-dose Al applications are based on projected longevity and P binding efficiencies presented in Table 10. Since there is uncertainty in projected longevity, lake and sediment monitoring will be an important component of adaptively managing the lake. For instance, as more Al is layered on top of the sediment, P binding efficiency and longevity may increase, resulting in less frequent low-dose Al applications.

ACKNOWLEDGMENTS:

H. Lieffort and L. Provos are gratefully acknowledged for their participation in field and laboratory analyses. Funding was provided by the City of Eau Claire, WI, and the Wisconsin Department of Natural Resources. Phil Fieber, Director, Parks, Recreation, and Forestry, for the City of Eau Claire, and Patrick Sorge, Limnologist, for the Wisconsin DNR, were project managers.

REFERENCES:

Ameel JJ, Axler RP, Owen CJ. 1993. Persulfate digestion for determination of total nitrogen and phosphorus in low nutrient water. American Environmental Laboratory (October, 1993):8-10.

American Public Health Association. 2005. Standard methods for the examination of water and wastewater. 21th ed., Washington, DC.

Carlson RE. 1977. A trophic state index for lakes. Limnol. Oceanogr. 22:361-369.

de Vicente I, Jensen HS, Andersen FØ. 2008a. Factors affecting phosphate adsorption to aluminum in lake water: Implications for lake restoration. Sci Total Environ 389:29-36.

de Vicente I, Huang P, Andersen FØ, Jensen HS. 2008b. Phosphate adsorption by fresh and aged aluminum hydroxide. Consequences for lake restoration. Environ Sci Technol 42:6650-6655.

Håkanson L, Jansson M. 2002. Principles of lake sedimentology. The Blackburn Press, Caldwell, NJ USA.

Hjieltjes AH, Lijklema L. 1980. Fractionation of inorganic phosphorus in calcareous sediments. J. Environ. Qual. 8: 130-132.

Johnson JA. 2010. Evaluation of lake-wide, early-season herbicide treatments for controlling invasive curlyleaf pondweed (*Potamogeton crispus*) in Minnesota Lakes. Master's thesis, University of Minnesota.

Johnson JA, Jones AR, Newman RM. 2012. Evaluation of lakewide, early season herbicide treatments for controlling invasive curlyleaf pondweed (*Potamogeton crispus*) in Minnesota Lakes. Lake Reserv Manage 28:346-363.

Jones JR, Obrecht DV, Thorpe AR. 2011. Chlorophyll maxima and chlorophyll:total phosphorus ratios in Missouri reservoirs. Lake Reserv Manage 27:321-328.

Lewandowski J, Schauser I, Hupfer M. 2003. Long term effects of phosphorus precipitations with alum in hypereutrophic Lake Süsser See (Germany). Wat Res 37:3194-3204.

Madsen JD. 1993. Biomass techniques for monitoring and assessing control of aquatic vegetation. Lake Reserv Manage 7:141-154.

Middelboe AL, Markager S. 1997. Depth limits and minimum light requirements of freshwater macrophytes. Freshwat. Biol. 37:553-568.

Nürnberg GK. 1988. Prediction of phosphorus release rates from total and reductant-soluble phosphorus in anoxic lake sediments. Can J Fish Aquat Sci 45:453-462.

Psenner R, Puckso R. 1988. Phosphorus fractionation: Advantages and limits of the method for the study of sediment P origins and interactions. Arch Hydrobiol Biel Erg Limnol 30:43-59.

Welschmeyer NA. 1994. Fluorometric analysis of chlorophyll a in the presence of chlorophyll b and pheopigments. Limnol. Oceanogr. 39:1985-1992.

Woolf TE, Madsen JD. 2003. Seasonal biomass and carbohydrate allocation patterns in southern Minnesota curlyleaf pondweed populations. J Aquat Plant Manage 41:113-118.

Table 1. Typical water column depths at the various water sampling stations in Half Moon Lake, Wisconsin.

Station	Nominal Depth	
	(m)	(ft)
10	3.0	9.8
20	3.0	9.8
30	2.5	8.2
40	2.5	8.2
50	2.2	7.2
60	1.8	5.9

Table 2. Mean summer (Jul-Sep) post-alum treatment concentrations of total phosphorus (P), viable chlorophyll (CHLA), Secchi disk transparency, and the light attenuation coefficient (k_d) at various stations in Half Moon Lake in 2016

	2016			
Station	Total P (mg/L)	CHLA (ug/L)	Secchi (m)	PAR (m^{-1})
10	0.049	48.4	0.9	1.4
20	0.046	48.7	0.9	1.6
30	0.042	37.4	1.0	1.4
40	0.040	33.2	1.0	1.3
50	0.038	24.2	1.2	1.3
60	0.030	5.8	2.0	0.9
Main arm	0.044	41.9	0.9	1.4

Table 3. Carlson and Wisconsin trophic State Index (TSI) values derived from mean total phosphorus (TP), viable chlorophyll (chla), and Secchi disk (SD) transparency for the post-alum treatment period (Jun-Sep) of 2016.

	2016					
	Carlson			Wisconsin		
Station	TSI_{TP}	TSI_{chla}	TSI_{sd}	TSI_{TP}	TSI_{chla}	TSI_{sd}
10	60	69	62	59	64	62
20	60	69	62	59	64	61
30	58	66	60	58	63	61
40	57	65	60	57	63	61
50	57	62	57	56	57	57
60	53	48	50	51	48	52
Main arm	59	67	61	58	63	61

Table 4. Comparison of mean summer flow in 1999 versus 2012-16 for various storm sewers draining into Half Moon Lake.

Sewer	Location		1999			2012			2013			2014			2015			2016	
			Precip	Flow		Precip	Flow		Precip	Flow		Precip	Flow		Precip	Flow		Precip	Flow	
			(inches)	(ft^3/s)	(m^3/s)	(inches)	(ft^3/s)	(m^3/s)	(inches)	(ft^3/s)	(m^3/s)	(inches)	(ft^3/s)	(m^3/s)	(inches)	(ft^3/s)	(m^3/s)	(inches)	(ft^3/s)	(m^3/s)
1	Owen Park Pumps	Total	9.6	1.220	0.0346	8.3	1.242	0.0352	9.3	2.898	0.0821	23.8	2.454	0.0695	24.2	2.766	0.0783	22.8	2.700	0.0760
		Storm Flow		0.048	0.0014		0.182	0.0052		0.157	0.0044		0.158	0.0045		0.148	0.0042		0.120	0.0038
		Base Flow		1.172	0.0332		1.058	0.0300		2.742	0.0777		2.296	0.0650		2.620	0.0742		2.580	0.0731
2	Near Midlefort Clinic			0.091	0.0026		0.022	0.0006		0.020	0.0006		0.090	0.0026		0.047	0.0013		0.046	0.0013
3	West of Beach			0.038	0.0011		0.046	0.0013		0.219	0.0062									
4	Carson Park						0.003	0.0001		0.007	0.0002		0.023	0.0006		0.010	0.0003		0.020	0.0004

Table 5. Summer flow-weighted total phosphorus (P) and soluble reactive P (SRP) for various storm sewers in 1999 and 2012-16. See text for an explanation of 2015 mean total P (bold red font).

Sewer	Description	1999		2012		2013		2014		2015		2016	
		Total P	SRP	Total P	SRP	Total P	SRP	Total P	SRP	Total P	SRP	Total P	SRP
		(mg/L)		(mg/L)		(mg/L)		(mg/L)		(mg/L)		(mg/L)	
1	Storm Flow	0.344	0.038	0.358	0.019	0.417	0.015	0.295	0.024	**0.166**	0.039	0.410	0.035
1	Base Flow	0.074	0.010	0.109	0.040	0.108	0.043	0.084	0.045	0.079	0.039	0.085	0.045
2	Storm Flow	0.149	0.044	0.096	0.011	0.098	0.022	0.102	0.026	0.089	0.017	0.121	0.015
3	Storm Flow	0.301	0.045	0.205	0.022	0.204	0.015						
4	Storm Flow					0.178	0.031	0.171	0.042	0.131	0.043	0.170	0.058

Table 6. Mean summer (JUN-SEP) total phosphorus (P) and soluble reactive P (SRP) loading for various storm sewers in 1999 and 2012-16.

Sewer	Description	1999		2012		2013		2014		2015		2016	
		Total P	SRP	Total P	SRP	Total P	SRP	Total P	SRP	Total P	SRP	Total P	SRP
		(kg/d)		(kg/d)		(kg/d)		(kg/d)		(kg/d)		(kg/d)	
1	Storm Flow	0.040	0.004	0.159	0.008	0.159	0.006	0.115	0.006	0.060	0.014	0.135	0.011
1	Base Flow	0.212	0.029	0.282	0.104	0.725	0.289	0.472	0.241	0.506	0.250	0.537	0.284
2	Storm Flow	0.033	0.010	0.005	0.001	0.005	0.001	0.023	0.005	0.010	0.002	0.013	0.002
3	Storm Flow	0.028	0.004	0.023	0.002	0.109	0.008						
4	Storm Flow					0.003	0.001	0.009	0.002	0.003	0.001	0.006	0.002

Table 7. Summer (JUN-SEP) mass loading of total phosphorus (P) and soluble reactive P (SRP) for various storm sewers in 1999 and 2012-16.

Sewer	Description	1999		2012		2013		2014		2015		2016	
		Total P	SRP	Total P	SRP	Total P	SRP	Total P	SRP	Total P	SRP	Total P	SRP
		(kg/summer)		(kg/summer)		(kg/summer)		(kg/summer)		(kg/summer)		(kg/summer)	
1	Storm Flow	4.89	0.54	19.29	1.02	19.18	0.69	13.88	0.71	7.29	1.71	16.29	1.39
1	Base Flow	25.67	3.47	34.14	12.53	87.73	34.93	57.08	29.22	61.28	30.25	64.96	34.39
2	Storm Flow	4.03	1.19	0.63	0.07	0.61	0.14	2.77	0.60	1.23	0.23	1.63	0.20
3	Storm Flow	3.43	0.51	2.77	0.30	13.22	0.97						
4	Storm Flow					0.37	0.06	1.07	0.19	0.41	0.13	0.68	0.23

Table 8. Estimated Al dosage and application areas for future control of internal P loading in Half Moon Lake. Al application strategy is to apply lower Al dosages at 2 to 5 year intervals for up to 10 years (see Table 9). The goal with this strategy is to maximize P binding onto the Al floc, increase internal P loading control and longevity, and reduce overall costs.

	West arm	East arm
P flux through Al floc (g/m^2 y)	0.4	0.1
Control period (y)	2-3	4-5
Al dose (g/m^2)	50	25
Treatment area (m^2)	113,156	88,235
Depth contour (ft)	10	7.5
Cost per treatment ($)	$47,300	$14,750

Table 9. Example Al application strategy for Half Moon Lake. The west arm is treated every 3 years with ~ 50 g Al/m^2 while the east arm is treated every 5-6 years with 25 g Al/m^2 (see Table 8). Sediment and water chemistry are monitored to provide adaptive management and decision-making support for adjusting dosage and application strategy.

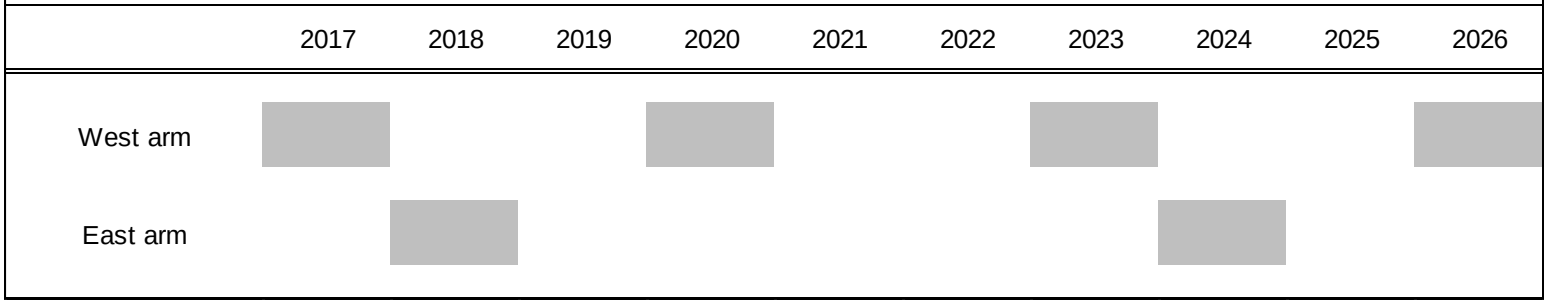

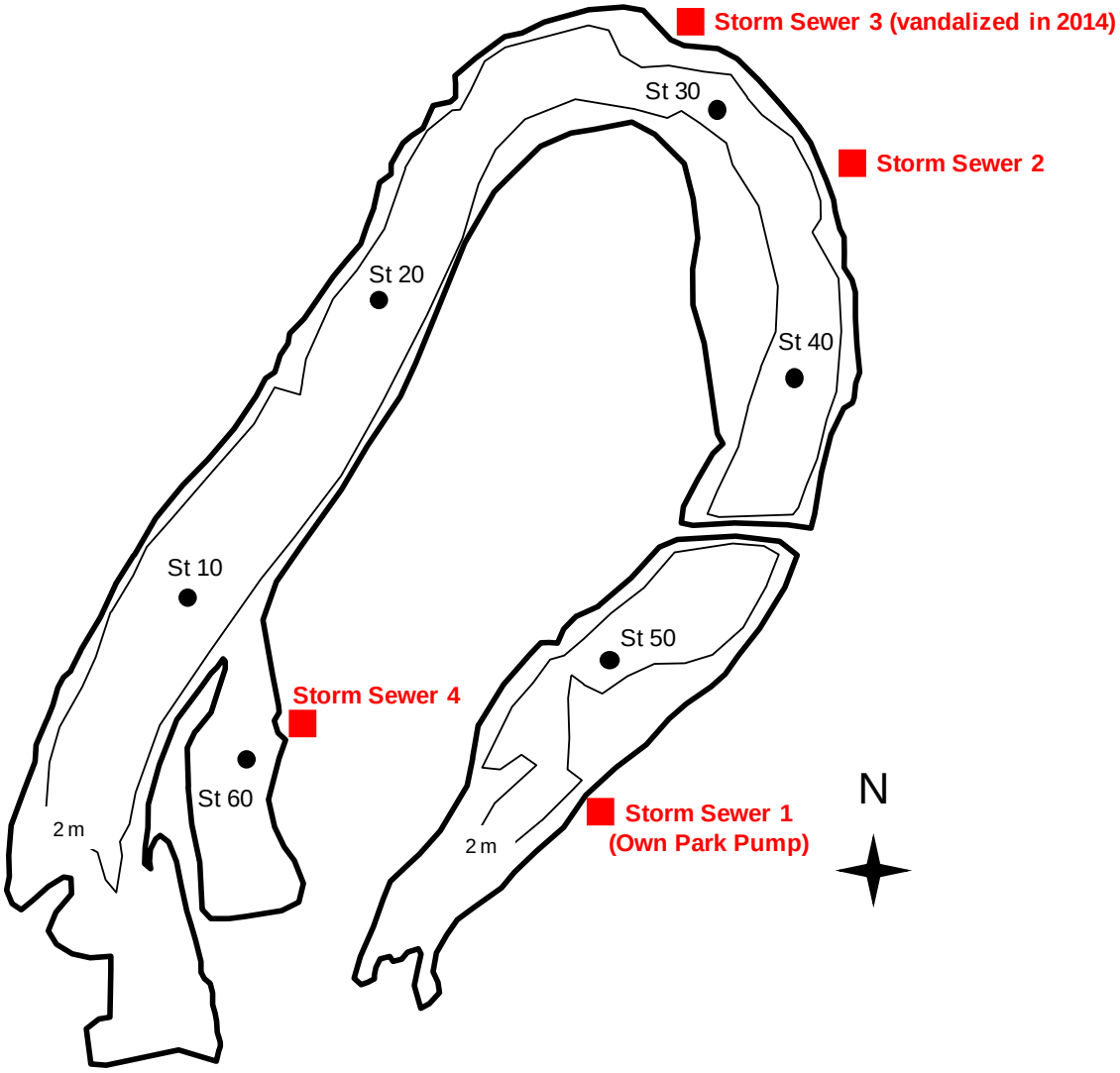

Figure 1. *Sampling station locations in Half Moon Lake.*

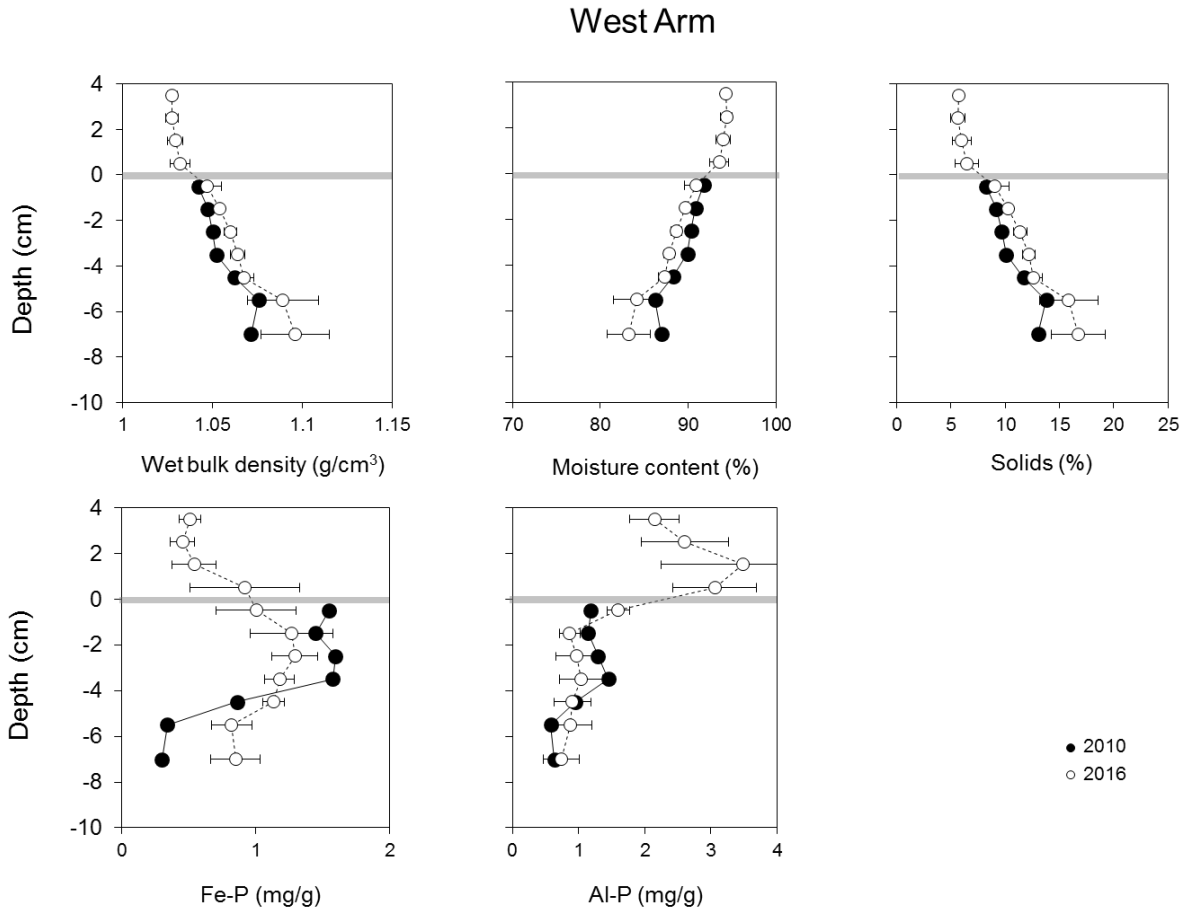

Figure 2. *Variations in sediment wet bulk density (upper left), moisture content (upper center), solids content (upper right), sediment iron-bound phosphorus (lower left), and aluminum-bound P (lower center) as a function of depth below the sediment-water interface for sediment cores collected at station 10 located in the west arm of Half Moon Lake. The year 2010 represents concentrations before alum treatment and the year 2016 represents conditions in July, four years after Al application. The horizontal gray line denotes the location of the original pretreatment surface sediment-water interface.*

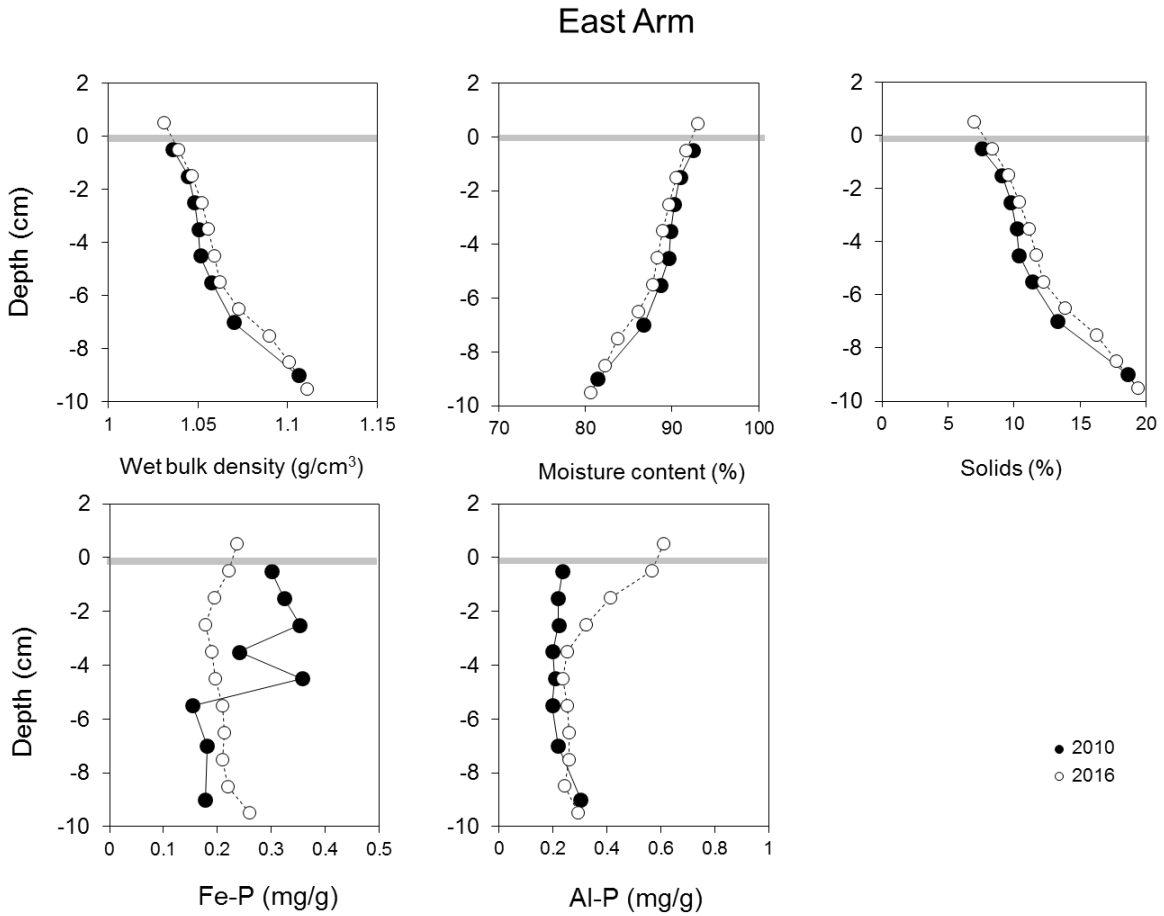

Figure 3. *Variations in wet bulk density (upper left), moisture content (upper center), solids content (upper right), iron-bound phosphorus (lower left), and aluminum-bound P (lower right) as a function of depth below the sediment-water interface for cores collected at station 30 located in the east arm of Half Moon Lake. The year 2010 represents concentrations before alum treatment and the year 2016 represents conditions in July, four years after Al application. The horizontal gray line denotes the location of the original pretreatment surface sediment-water interface.*

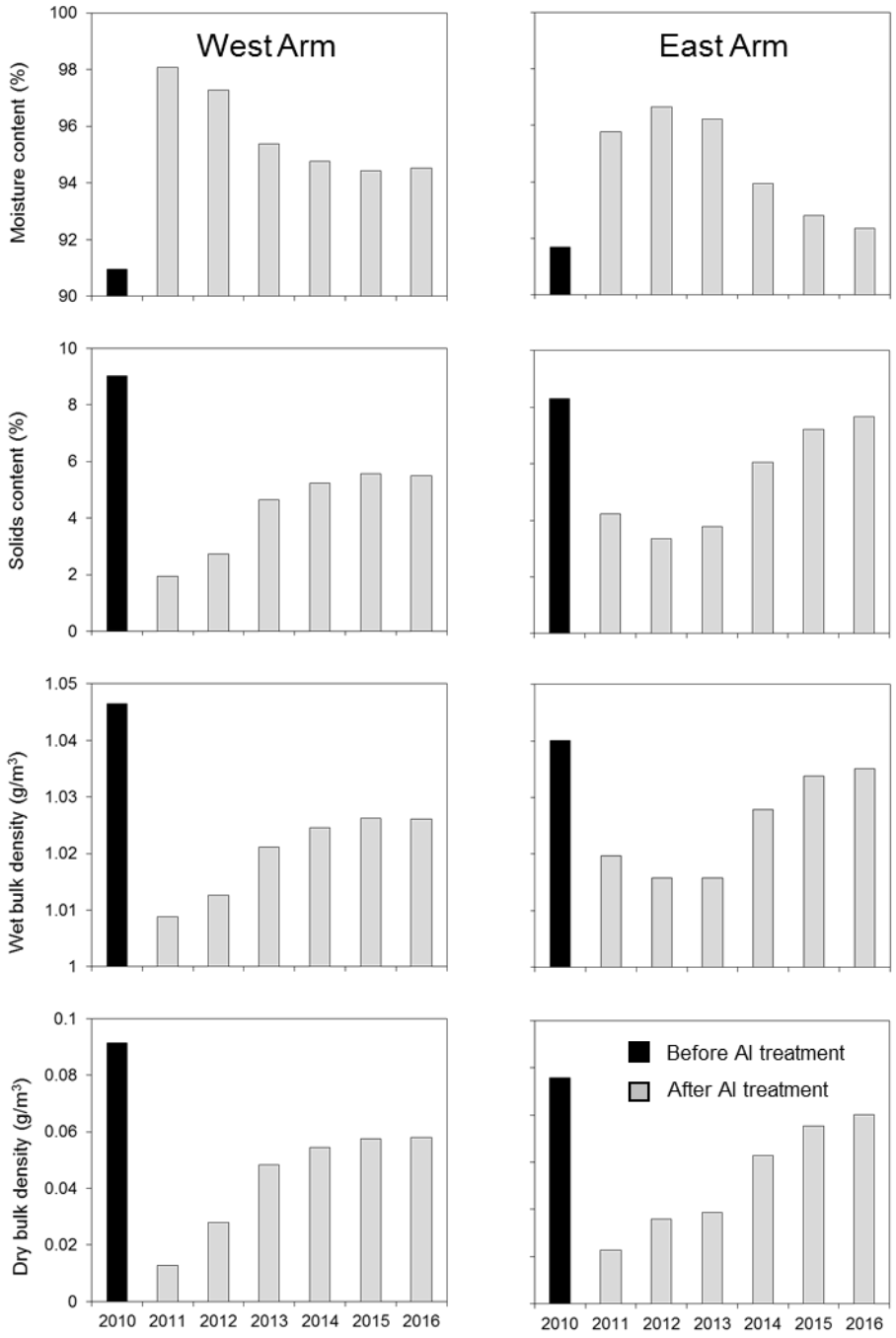

Figure 4. *Annual variations sediment physical-textural characteristics in the surface (upper 3 cm for the west arm and upper 1 cm for the east arm) sediment layer before and after Al treatment.*

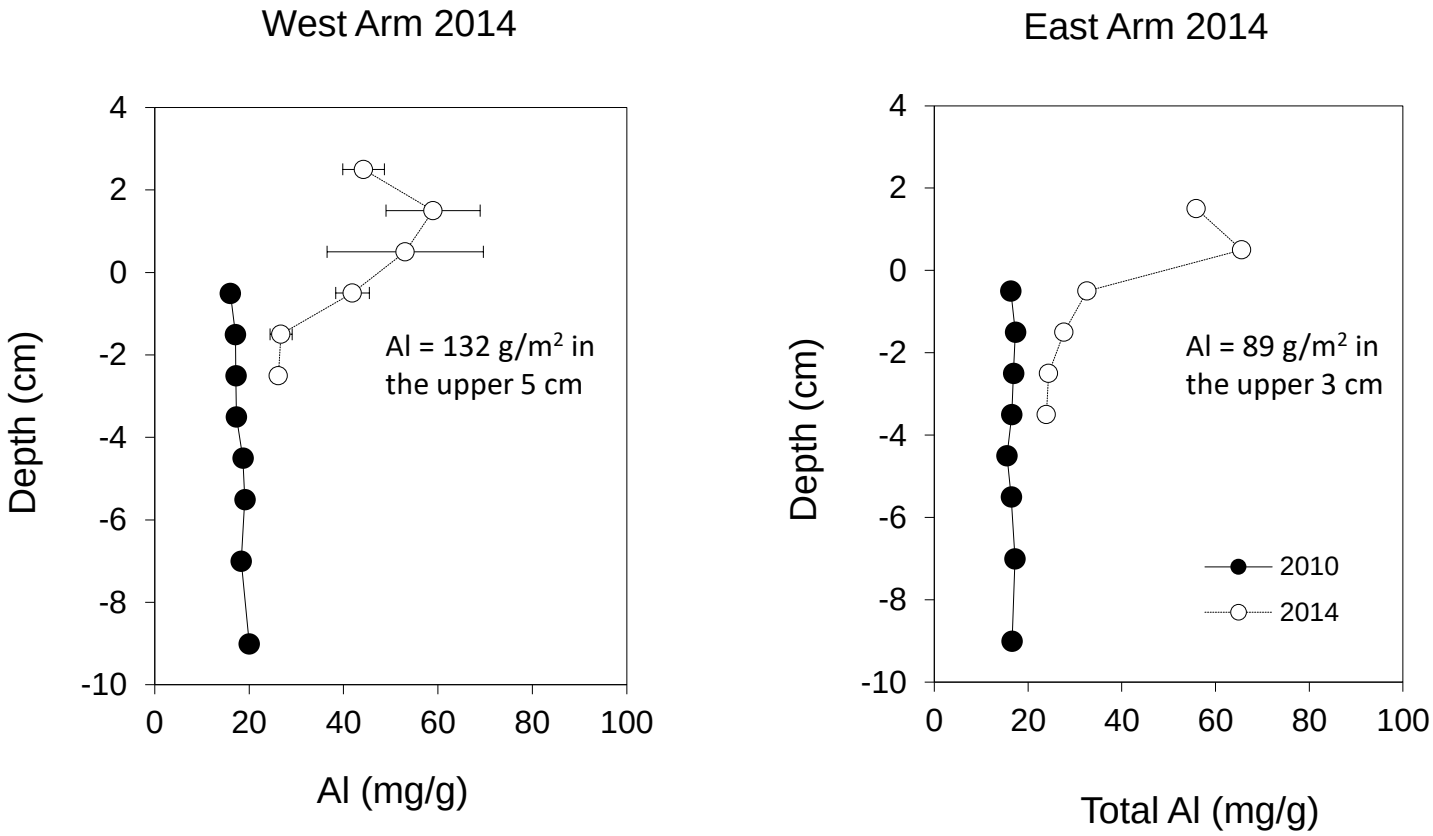

Figure 5. *Variations in aluminum (Al) as a function of depth below the sediment-water interface for cores collected at station 10 and 30. The year 2010 represents concentrations before alum treatment and the year 2014 represents conditions in July, three years after Al application.*

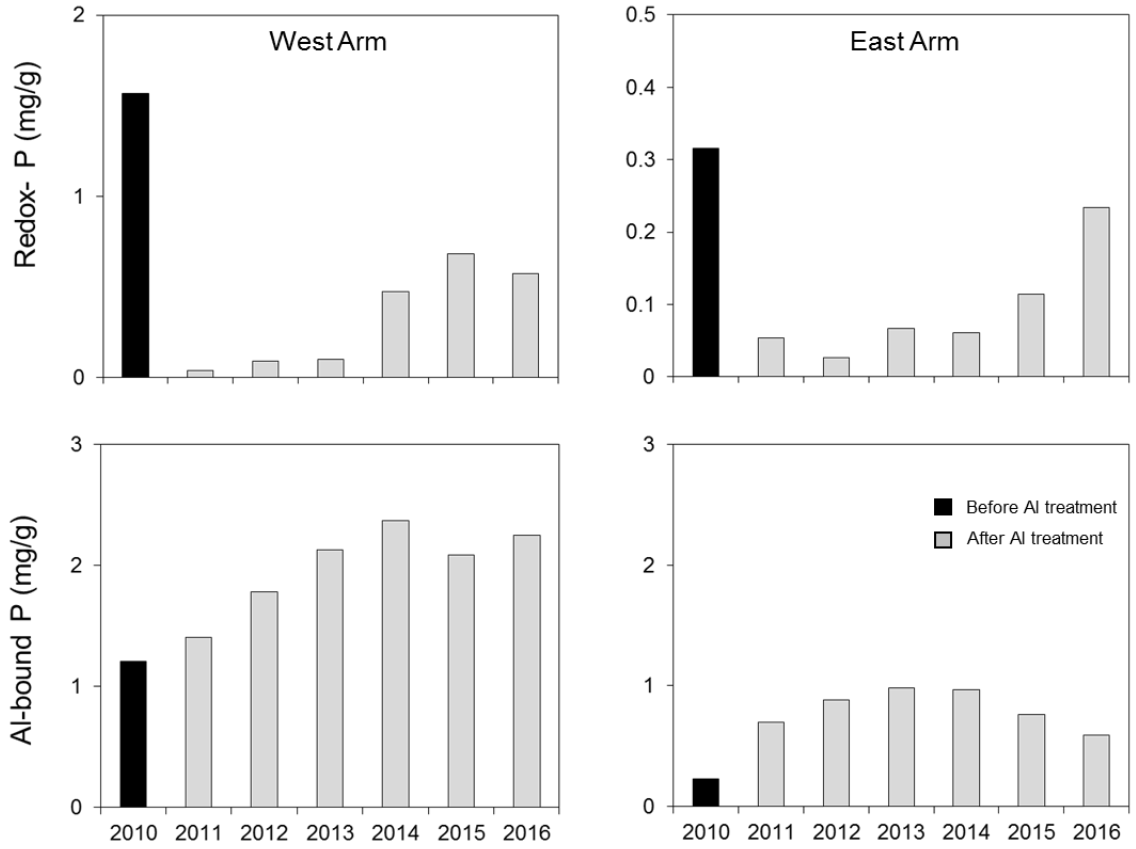

Figure 6. *Annual variations in redox-sensitive phosphorus (redox-P) and aluminum-bound P (Al-bound P) in the surface (upper 3 cm for the west arm and upper 1 cm for the east arm) sediment layer before and after Al treatment.*

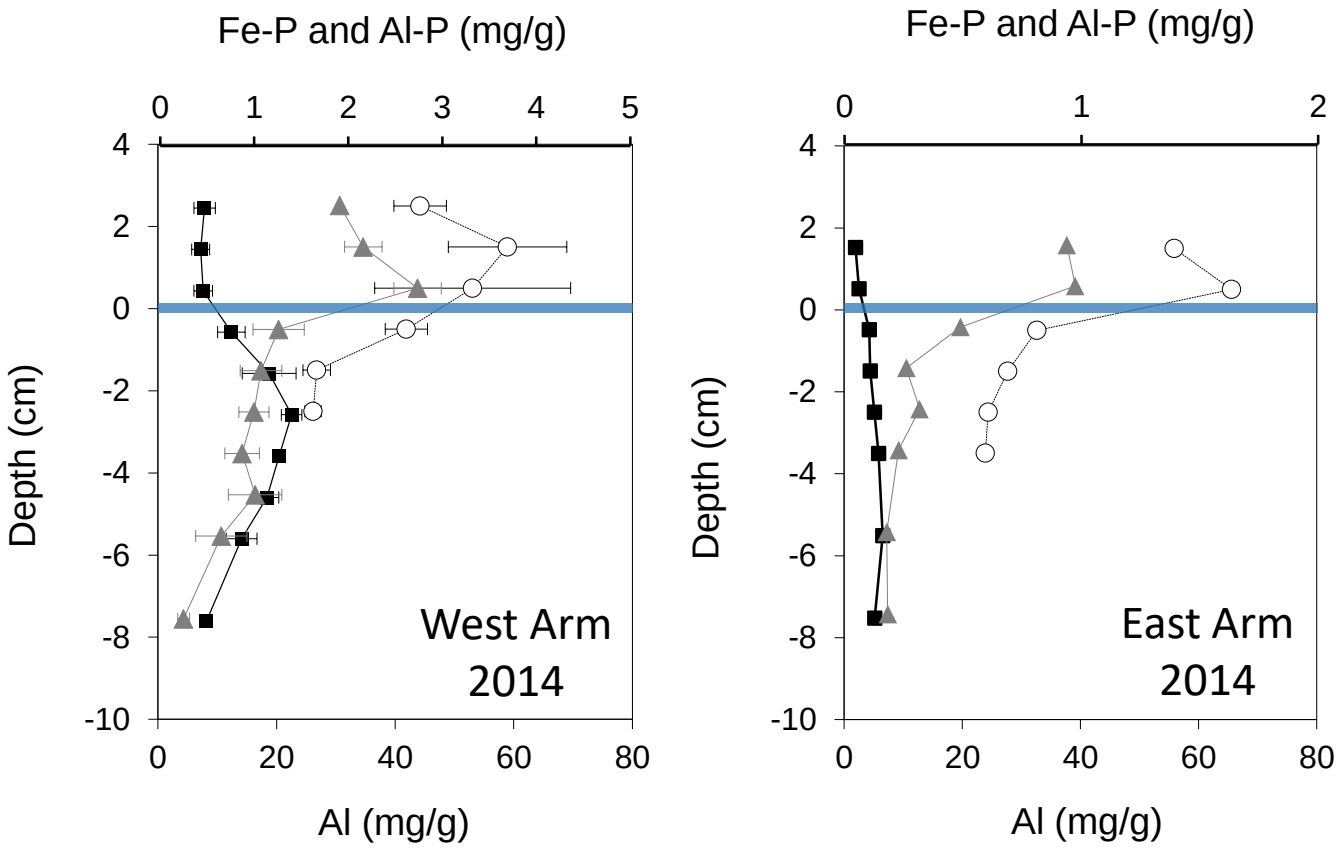

Figure 7. *A comparison of vertical variations in iron-bound phosphorus (Fe-P, squares), aluminum-bound P (triangles), and total aluminum (circles) in sediment cores collected in the west arm (station 10) and the east arm (station 30) in 2014. Horizontal blue line denotes the original sediment surface.*

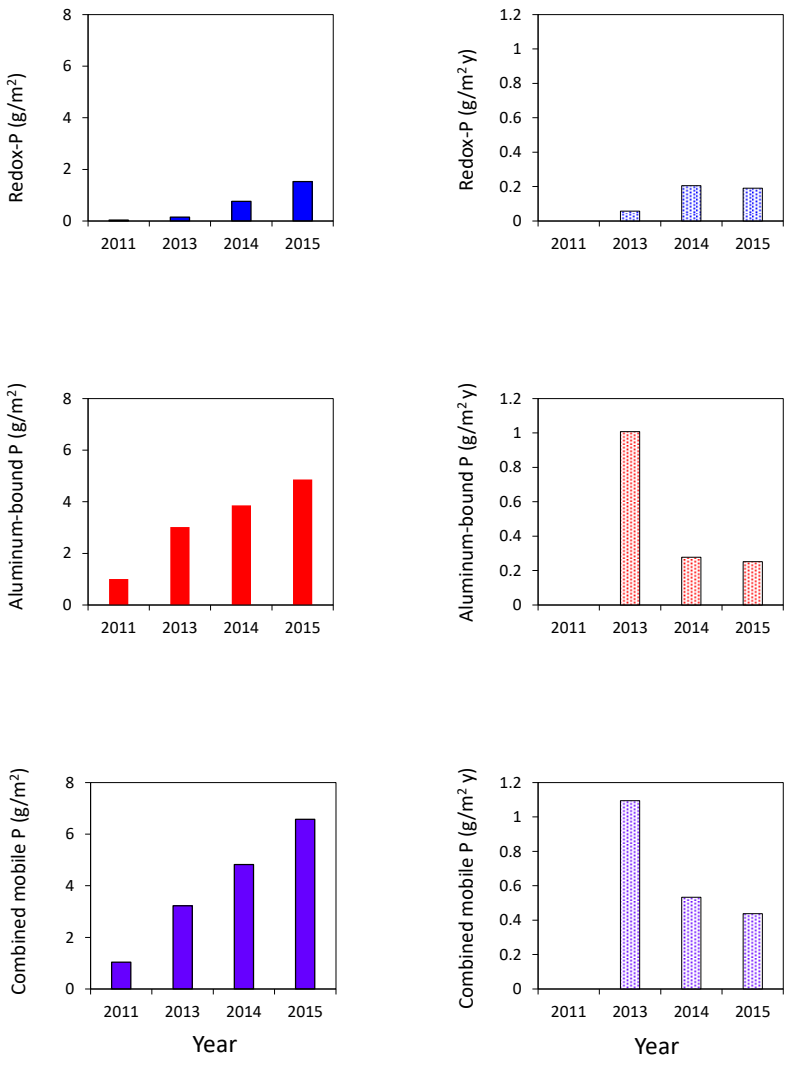

Figure 8. *Changes in the concentration (left panels) and rates of accumulation (right panels) of redox-sensitive phosphorus (redox-P), aluminum-bound P, and combined mobile P (i.e., the sum of redox-P and aluminum-bound P) in the Al floc layer (upper 3 cm) over time at station 10 (west arm sediment).*

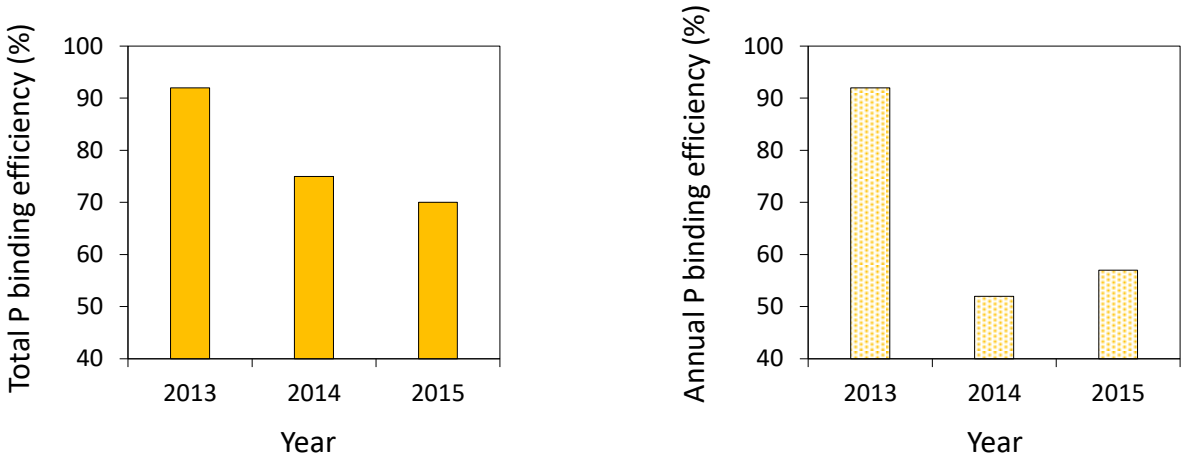

Figure 9. *Changes in total (i.e, current year minus 2011, left panel) and annual (i.e., between current and previous year) binding efficiency in the Al floc layer of station 10 (west arm) sediments.*

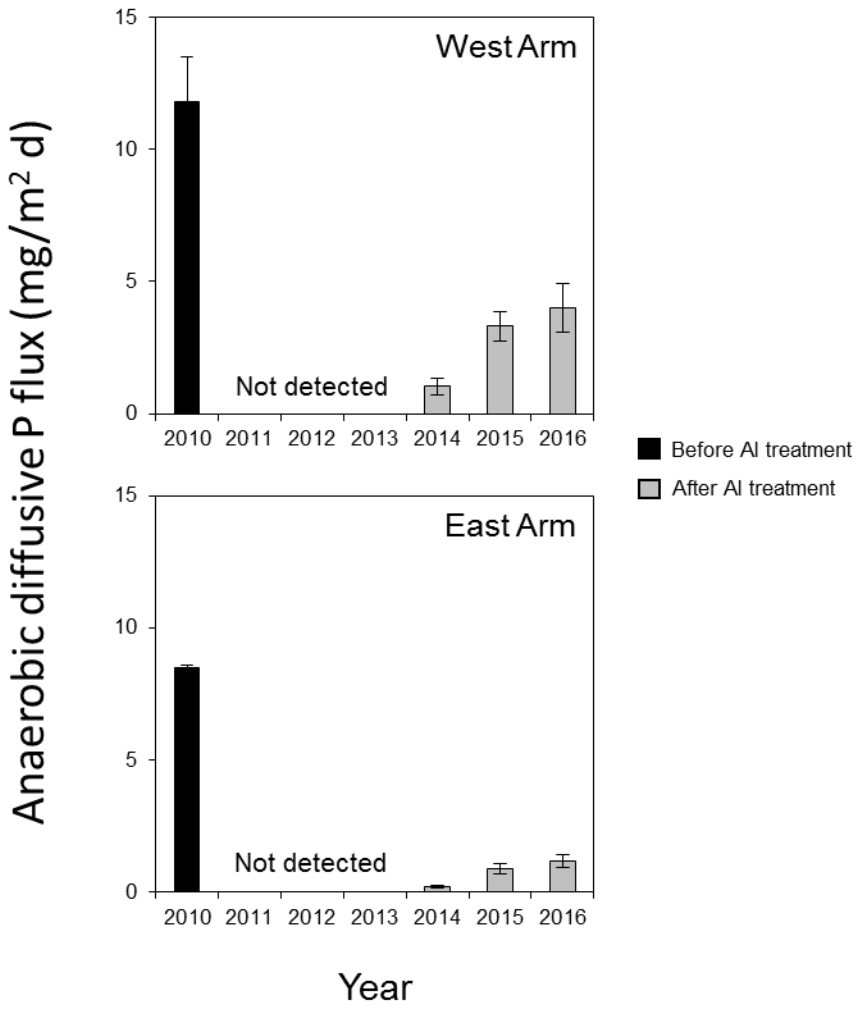

Figure 10. *Annual variations in the mean (n = 5) anaerobic phosphorus (P) release rate before and after Al treatment. Horizontal lines represent 1 standard error.*

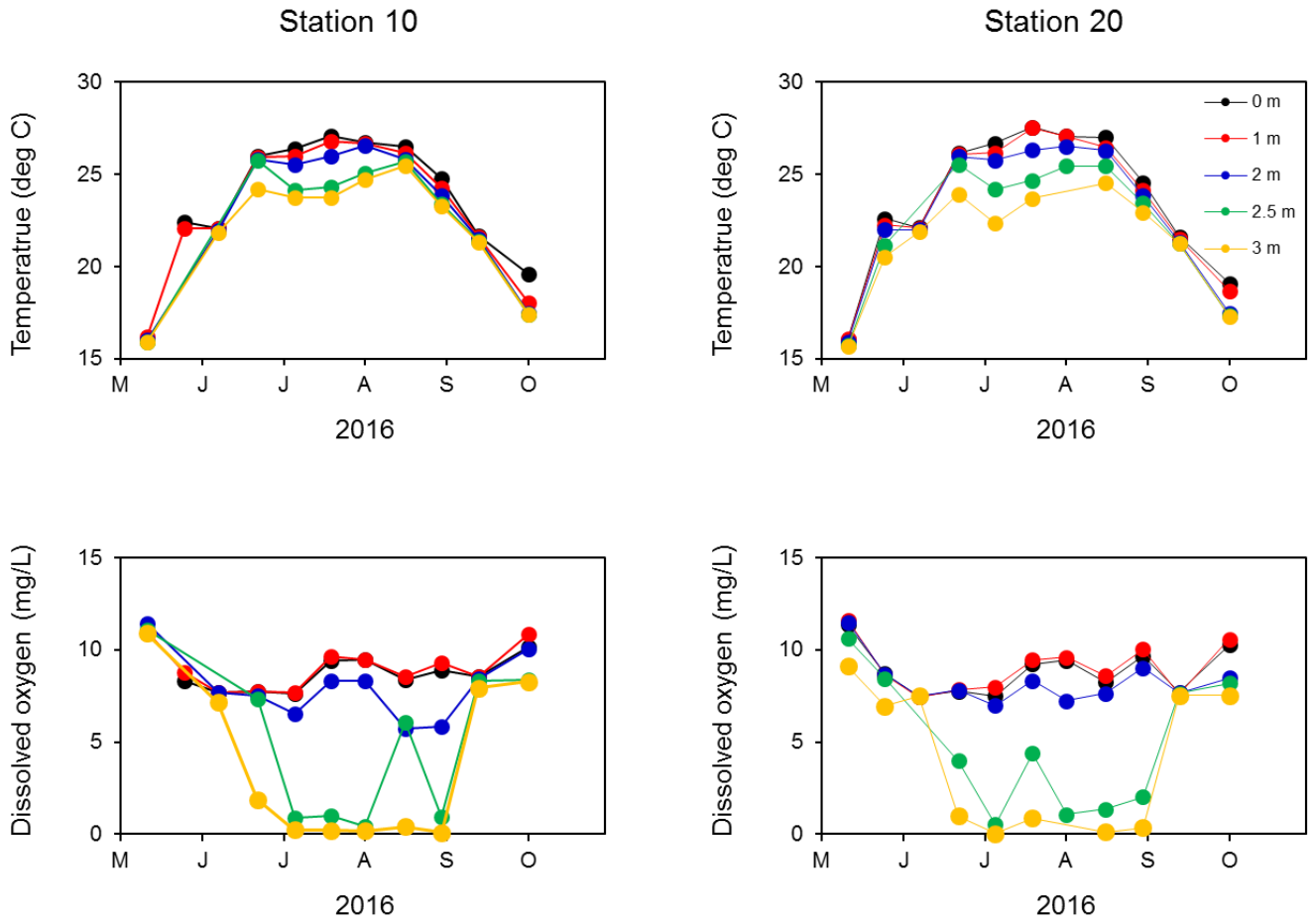

Figure 11. *Seasonal variations in water temperature and dissolved oxygen concentration at west arm stations 10 and 20 in Half Moon Lake in 2016.*

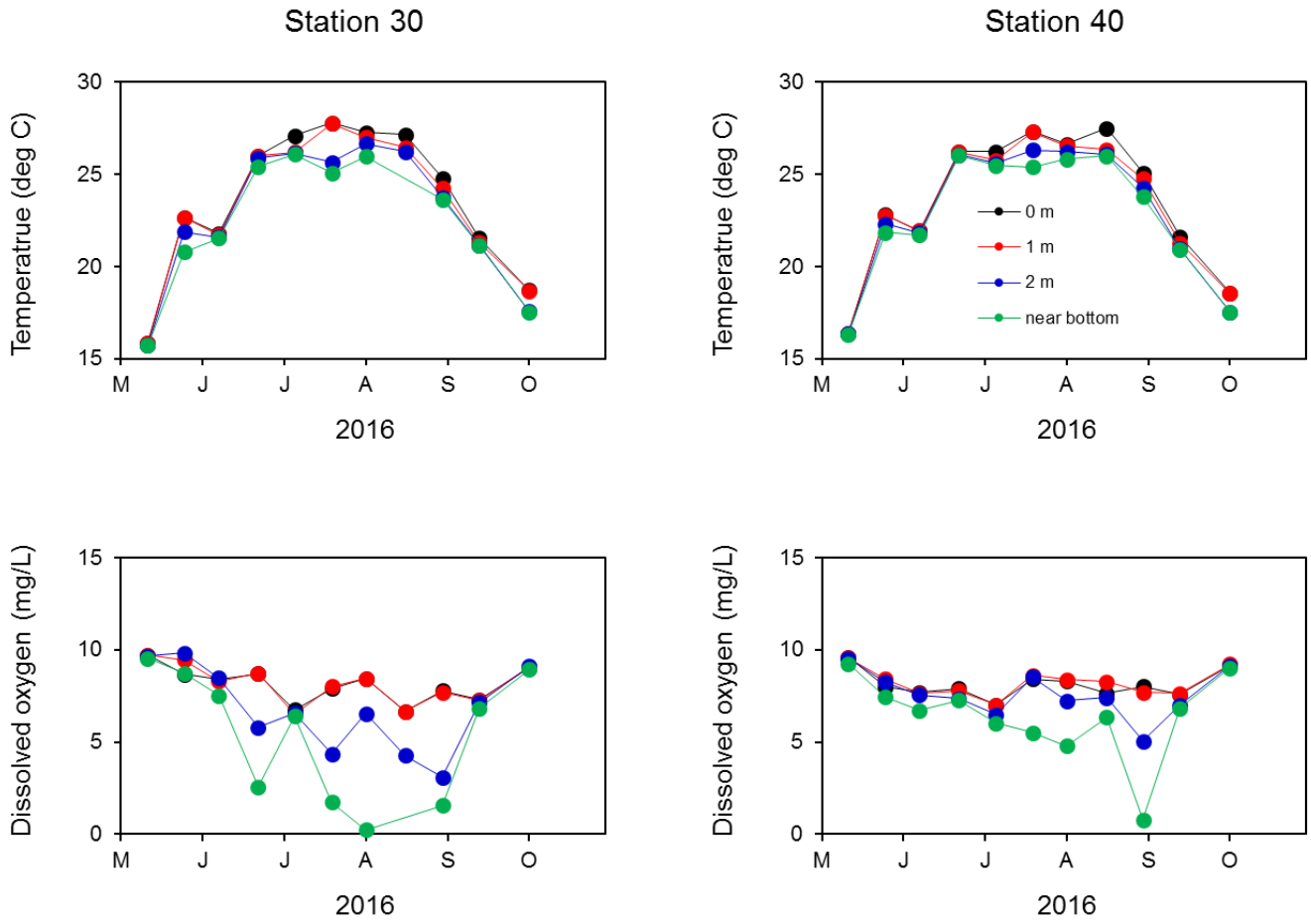

Figure 12. *Seasonal variations in water temperature and dissolved oxygen concentration at east arm stations 30 and 40 in Half Moon Lake in 2016.*

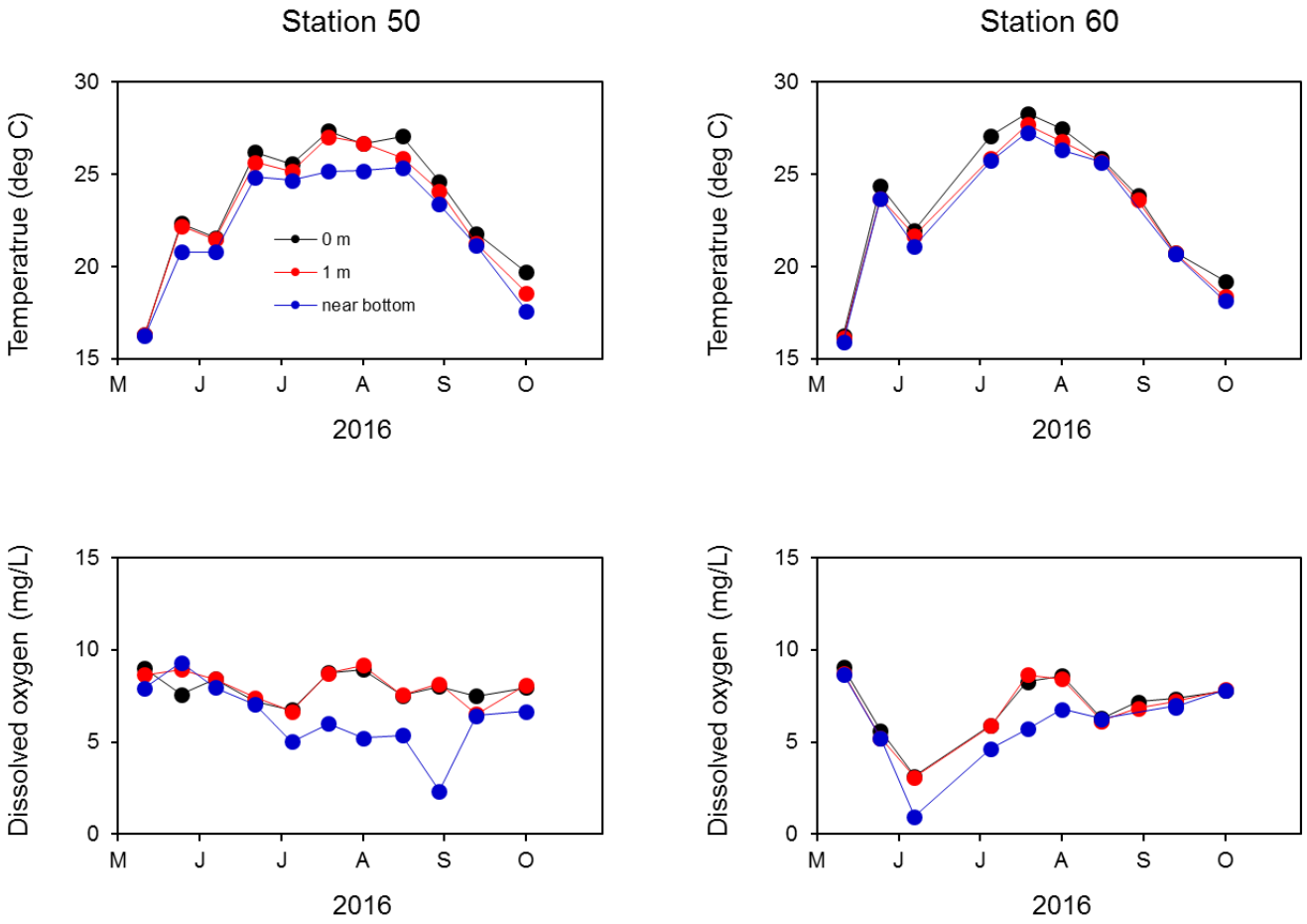

Figure 13. *Seasonal variations in water temperature and dissolved oxygen concentration at stations 50 and 60 in Half Moon Lake in 2016.*

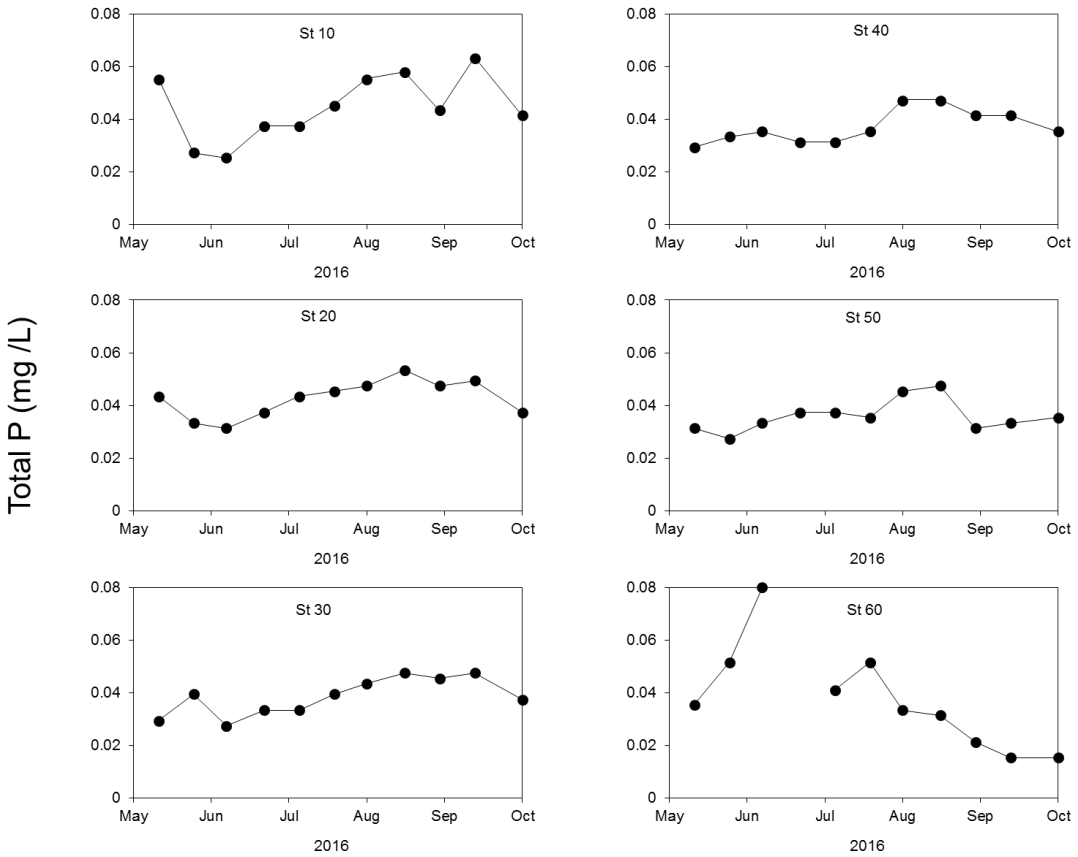

Figure 14. *Seasonal variations in total phosphorus (P) at various stations in Half Moon Lake in 2016.*

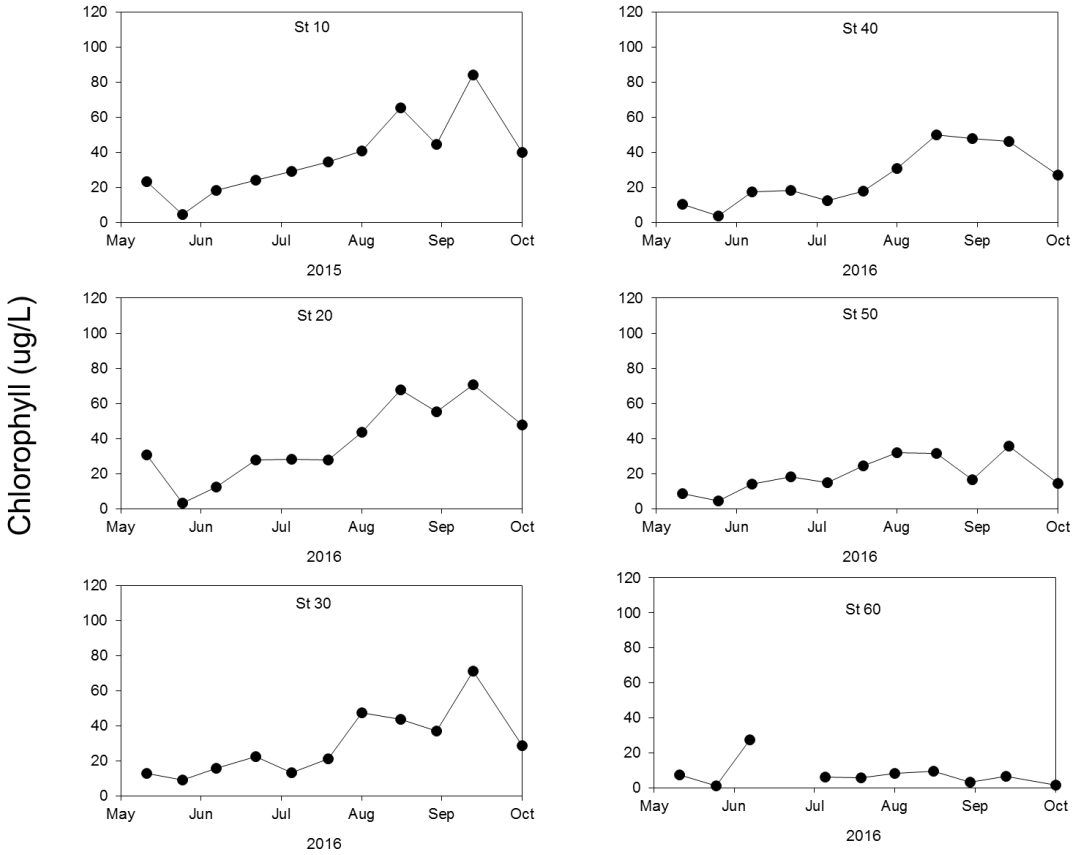

Figure 15. *Seasonal variations in chlorophyll at various stations in Half Moon Lake in 2016.*

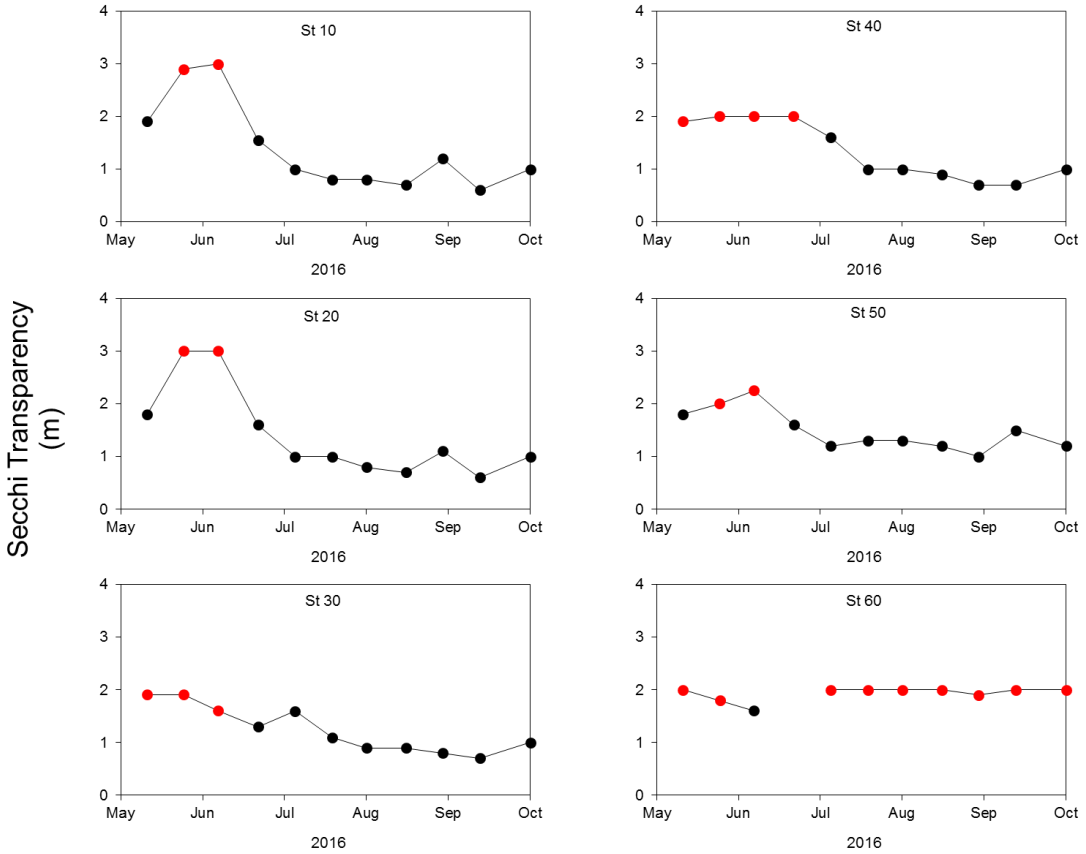

Figure 16. *Seasonal variations in Secchi disk transparency at various stations in Half Moon Lake in 2016. Red circles denote periods when Secchi disk transparency was equivalent to the lake bottom depth.*

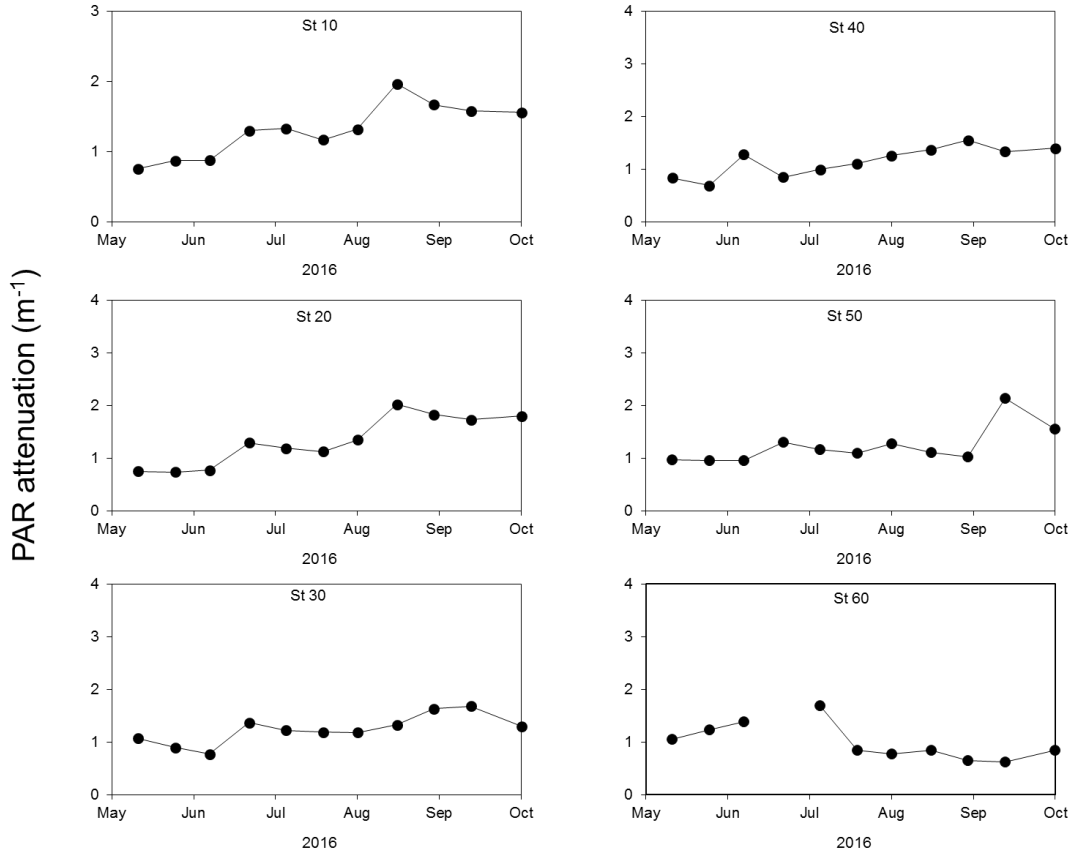

Figure 17. *Seasonal variations photosynthetically-active radiation (PAR) at various stations in Half Moon Lake in 2016.*

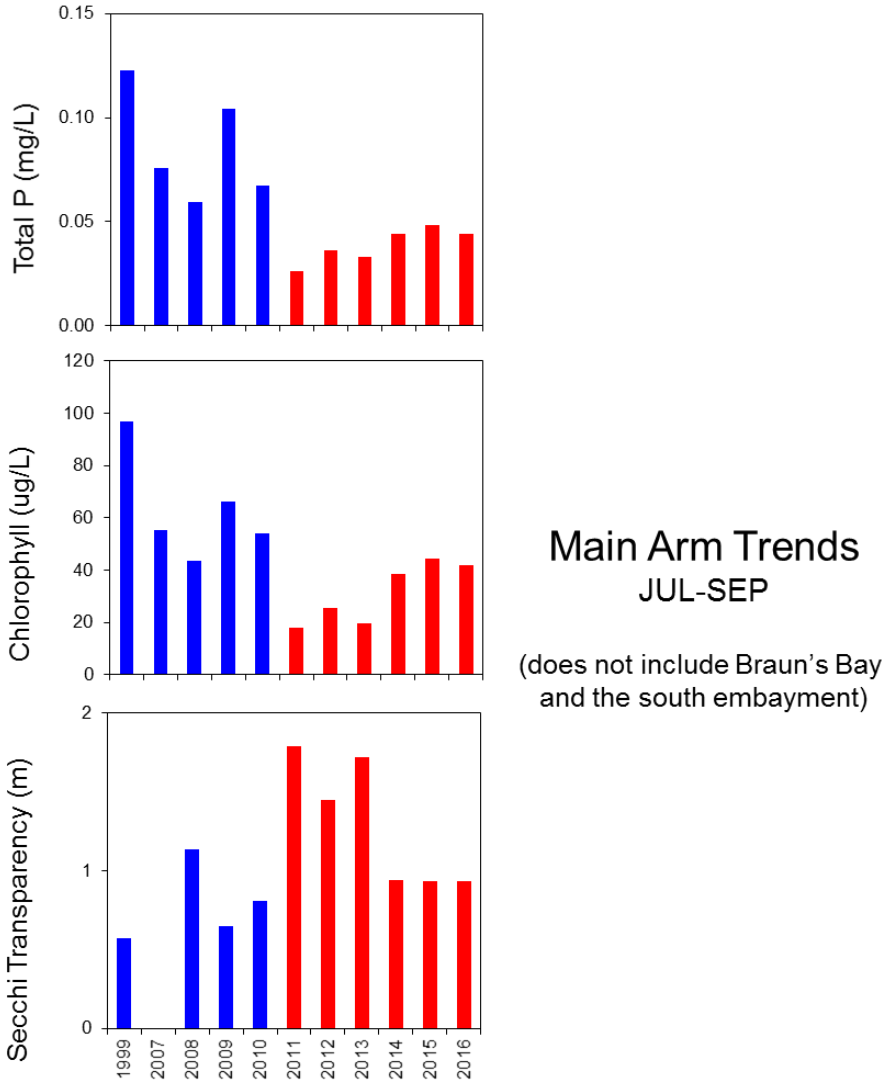

Figure 18. *Summer (JUL-SEP) mean total phosphorus (P), chlorophyll, and Secchi transparency in the main arm (i.e. west and east arms) of Half Moon Lake before (blue bars) and after (red bars) Al treatment (June, 2011).*

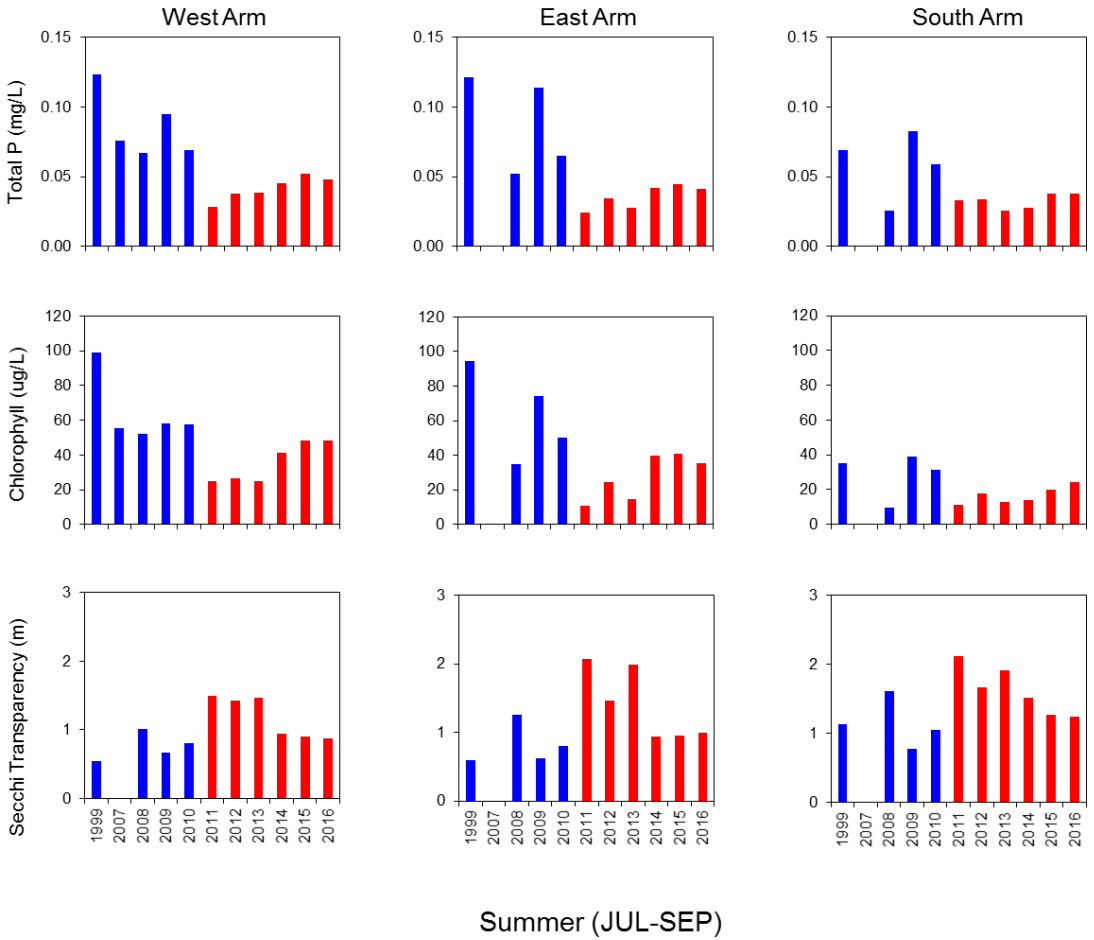

Figure 19. *Summer (JUL-SEP) mean total phosphorus (P), chlorophyll, and Secchi transparency in the west (i.e., station 10 and 20), east (i.e., station 30 and 40), and south (i.e., station 50) arms of Half Moon Lake before (blue bars) and after (red bars) Al treatment (June, 2011).*

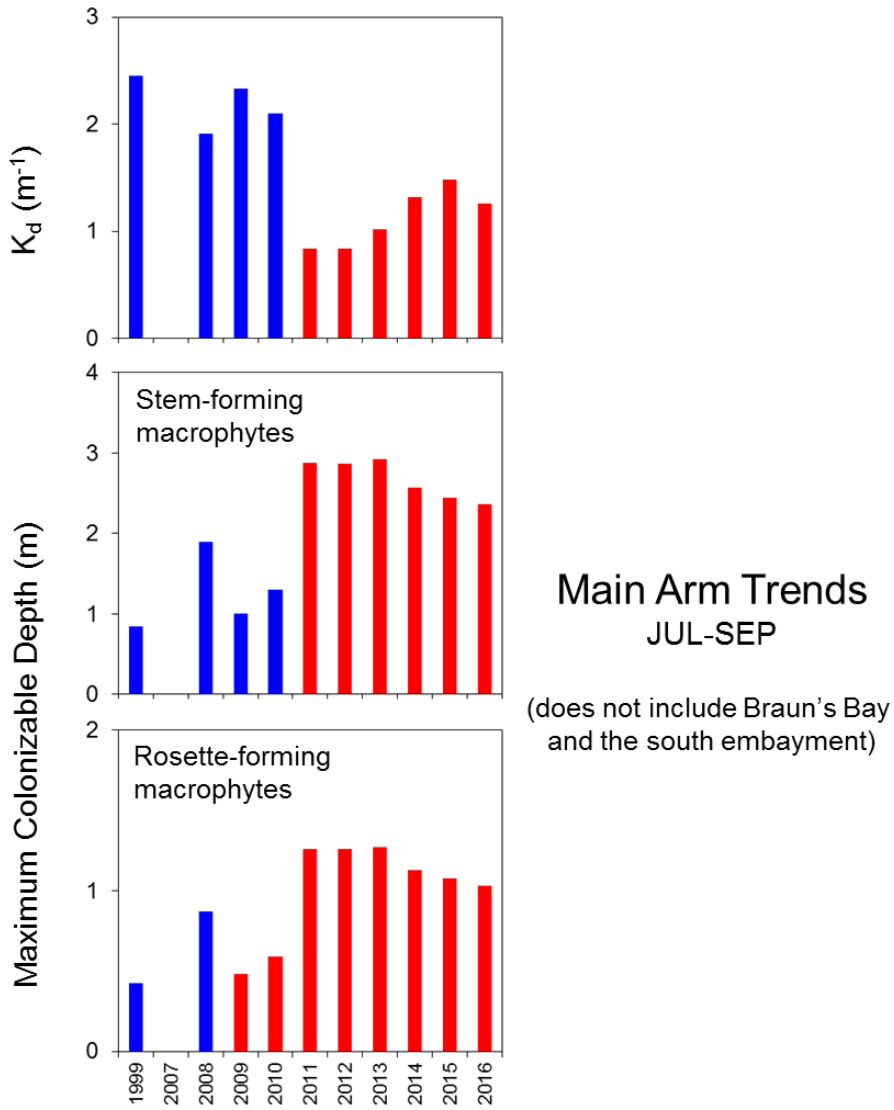

Figure 20. *Summer (JUL-SEP) mean maximum inhabitable depth for stem- and rosette-forming submersed aquatic macrophytes based on Middelboe and Markager (1997) in the main arm (i.e. west and east arms) of Half Moon Lake before (blue bars) and after (red bars) Al treatment (June, 2011).*

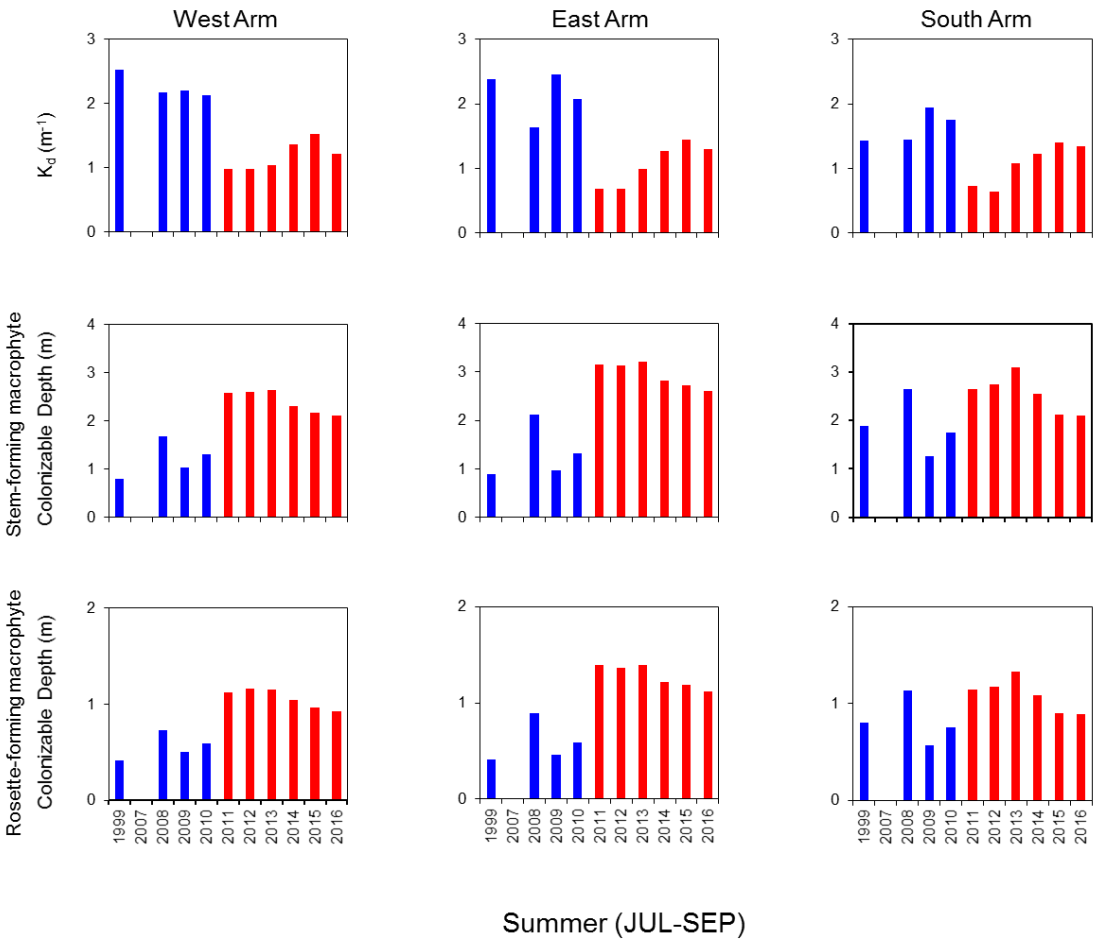

Figure 21. *Summer (JUL-SEP) mean maximum inhabitable depth for stem- and rosette-forming submersed aquatic macrophytes based on Middelboe and Markager (1997) in the west (i.e., station 10 and 20), east (i.e., station 30 and 40), and south (i.e., station 50) arms of Half Moon Lake before (blue bars) and after (red bars) Al treatment (June, 2011).*

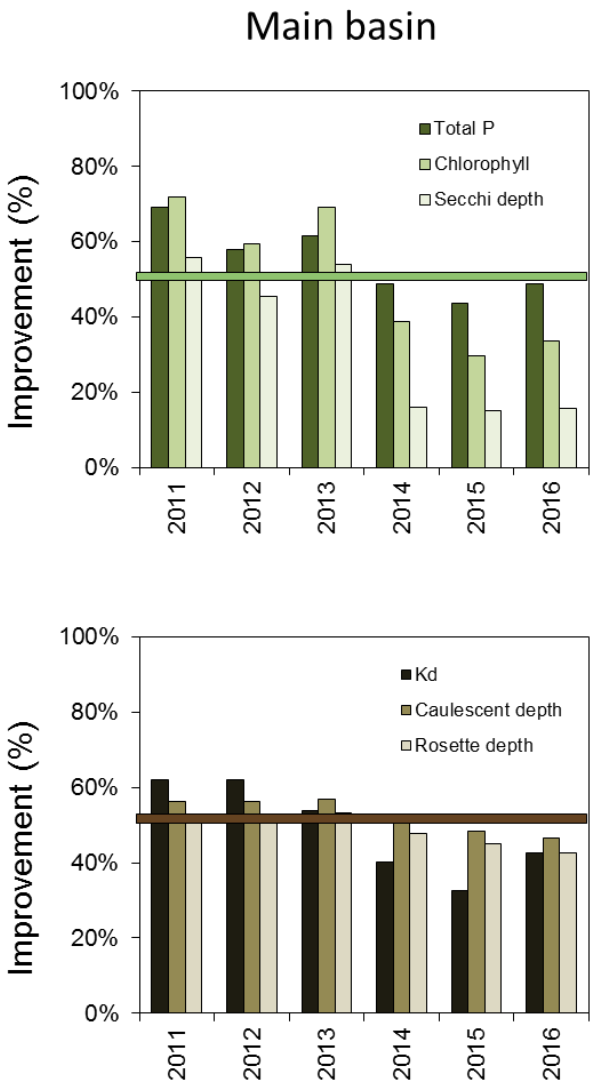

Figure 22. *Percent improvement (i.e., post-treatment reduction in mean total phosphorus and chlorophyll or increase in Secchi transparency) in mean summer (July-September) limnological response variables after application of alum in June, 2011) Horizontal bar denotes 50% improvement.*

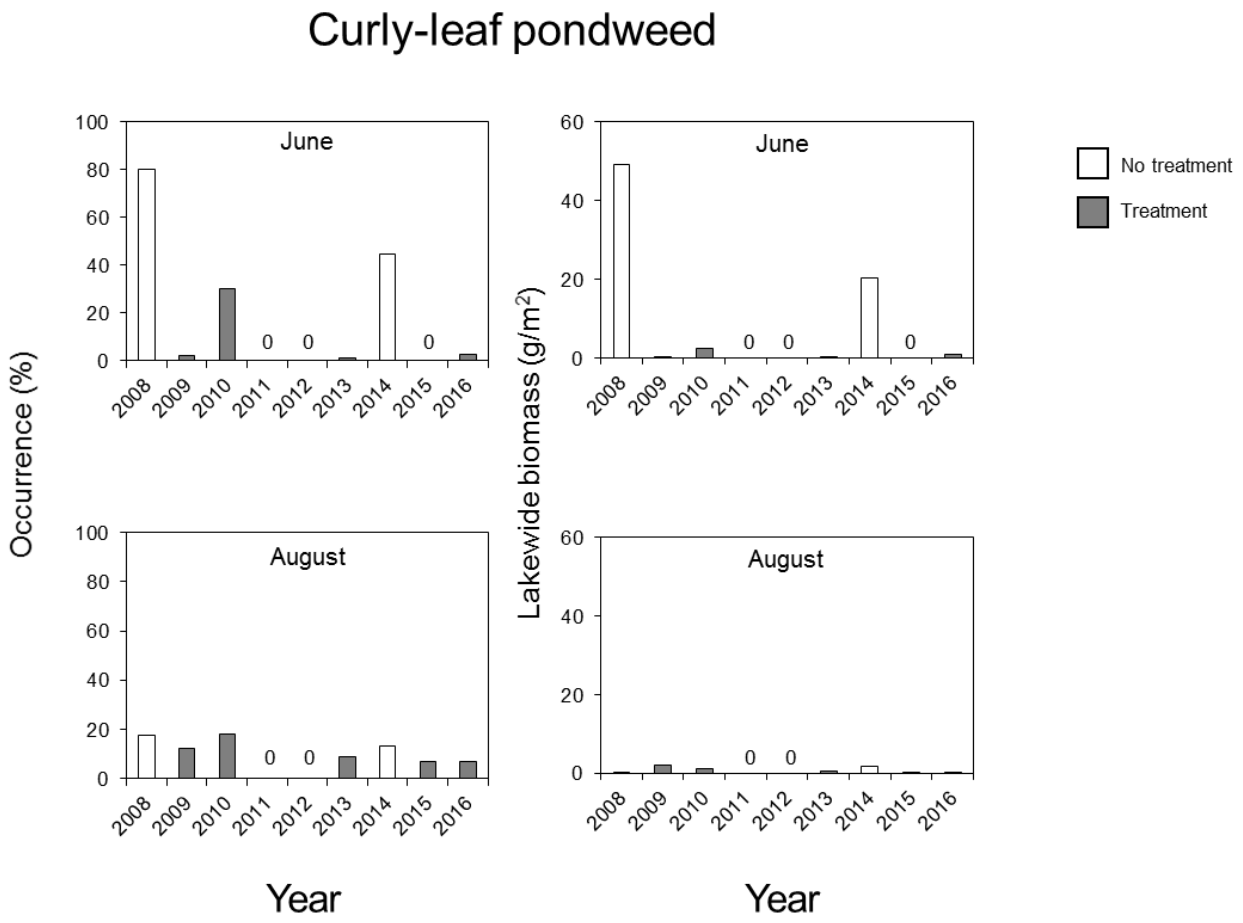

Figure 23. *Curly-leaf pondweed lake-wide mean biomass (n ~ 140-160) in June and August of various years. White columns represent means before the start of early spring Endothall treatments.*

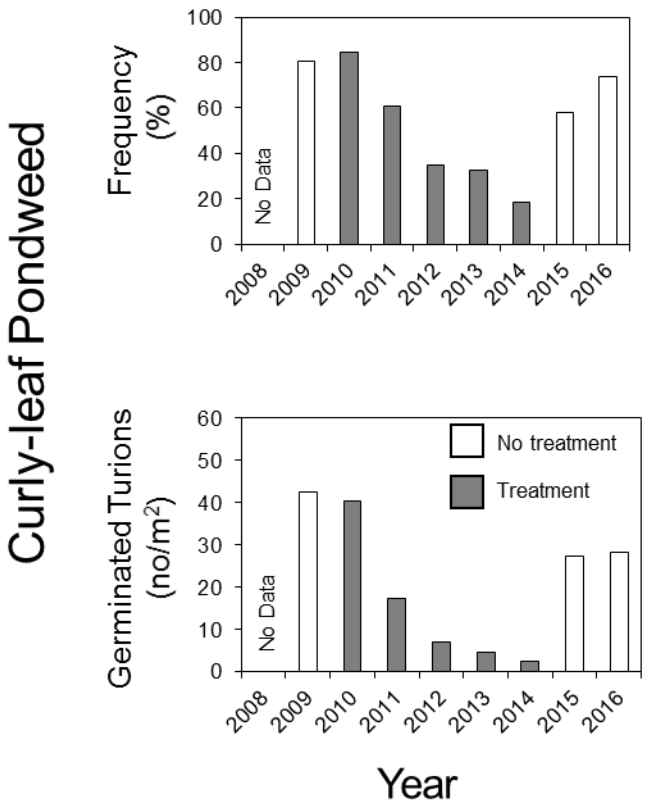

Figure 24. *Percent occurrence (n ~ 140-160; upper panel) and numbers (lower panel) of germinated curly-leaf pondweed tuions in April of various years. White columns represent means before the start of early spring Endothall treatments.*

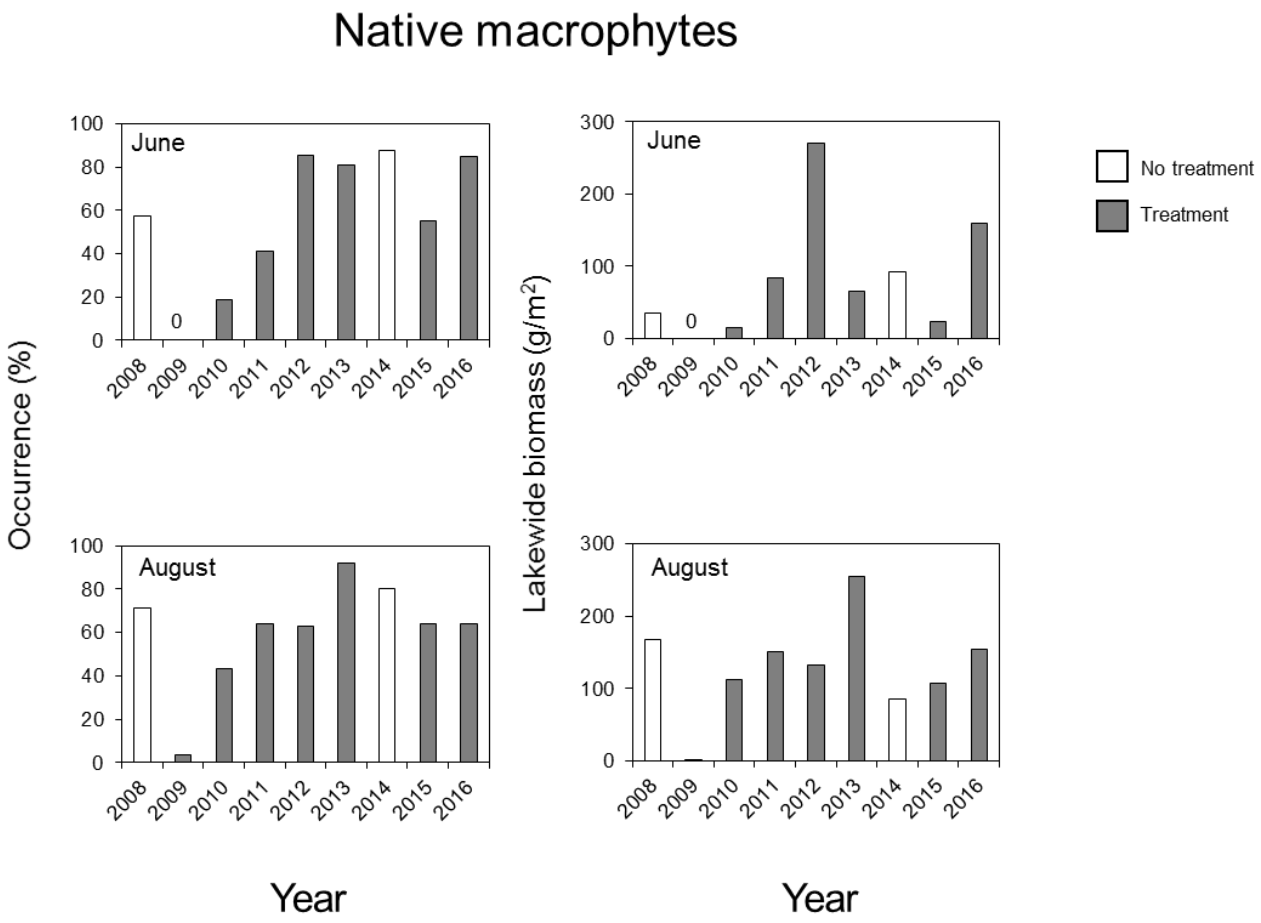

Figure 25. *Native submersed macrophyte lake-wide mean biomass (n ~ 140-160) in June and August of various years. 2008 was the pretreatment year. The pretreatment native macrophyte community in 2008 was dominated by coontail while elodea has dominated the post-treatment assemblage.*

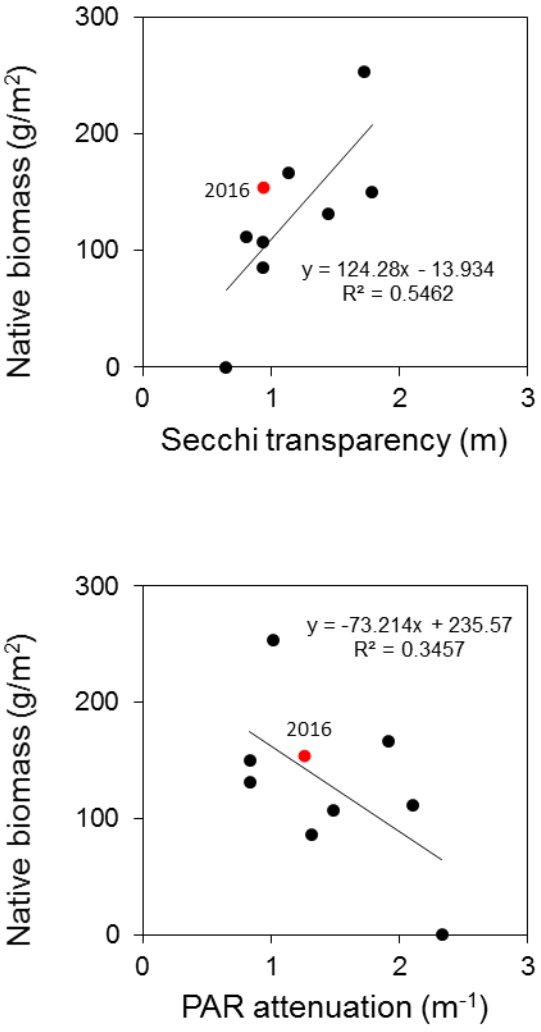

Figure 26. *Regression relationships between mean summer Secchi transparency (upper panel) or the mean summer photosynthetically active radiation (PAR) attenuation coefficient (lower panel) and mean native macrophyte biomass. Red circle denotes 2016.*

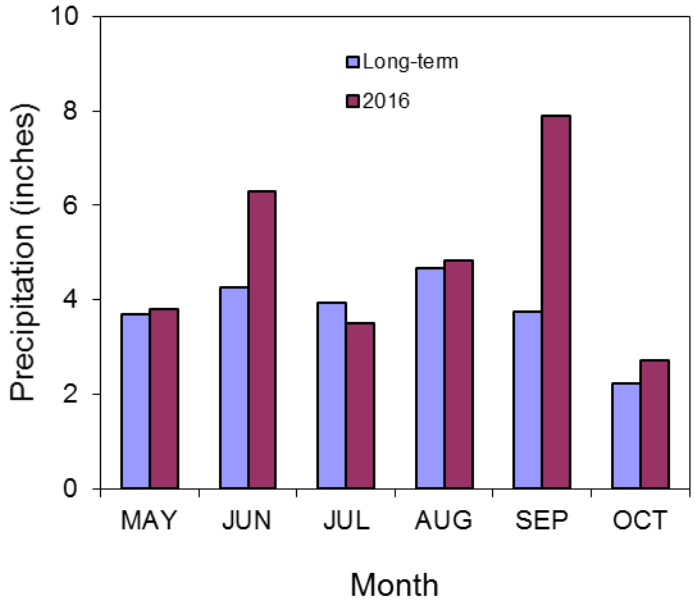

Figure 27. *Mean monthly precipitation measured at the Eau Claire Airport.*

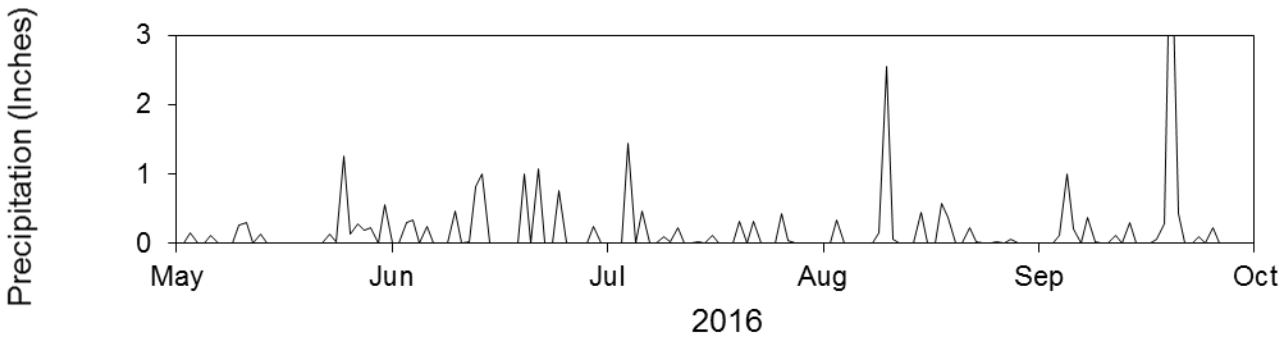

Figure 28. *Variations in daily precipitation in 2016.*

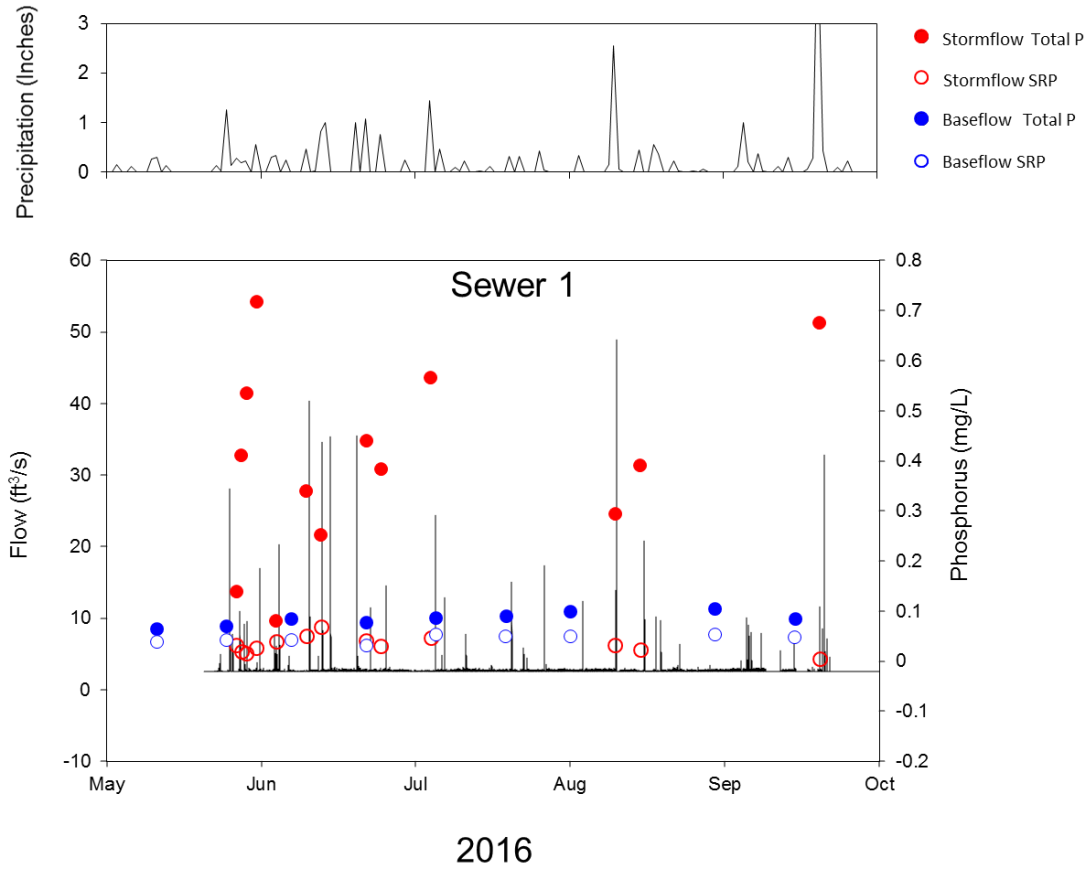

Figure 29. *Variations in flow and phosphorus concentrations for storm sewer 1 in 2016.*

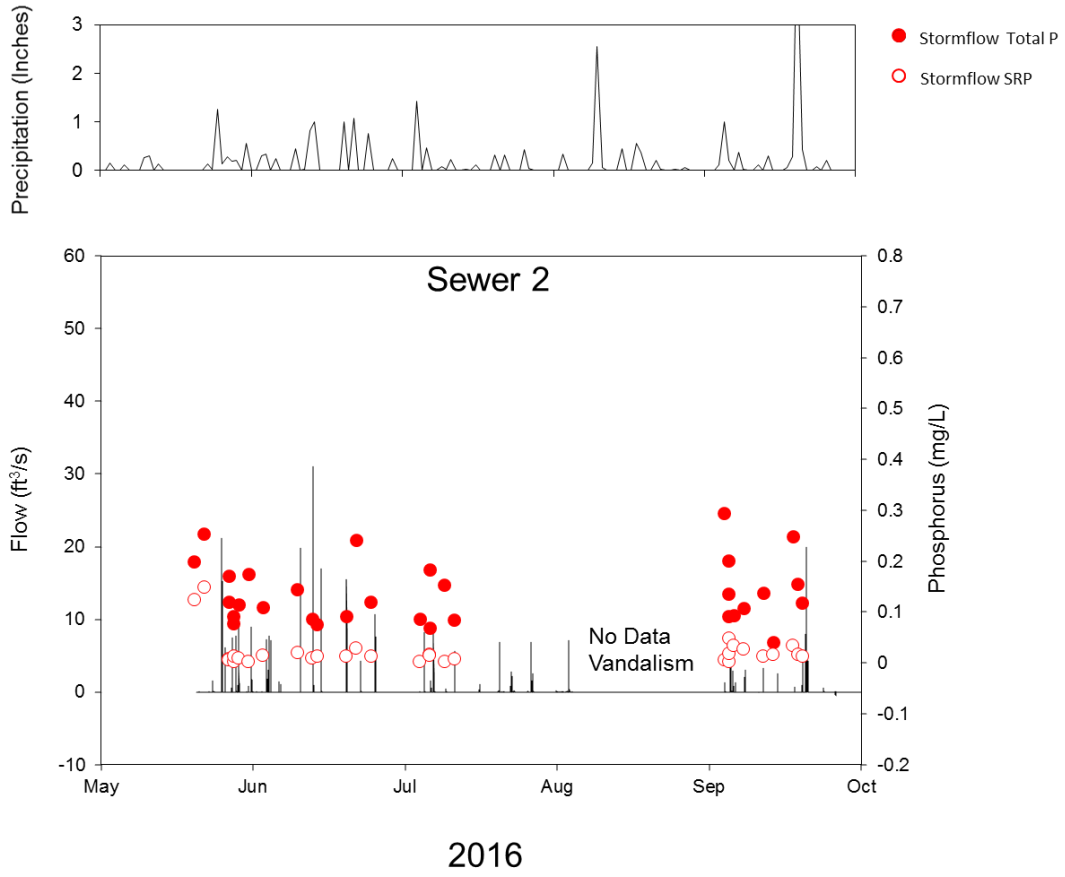

Figure 30. *Variations in flow and phosphorus concentrations for storm sewer 2 in 2016.*

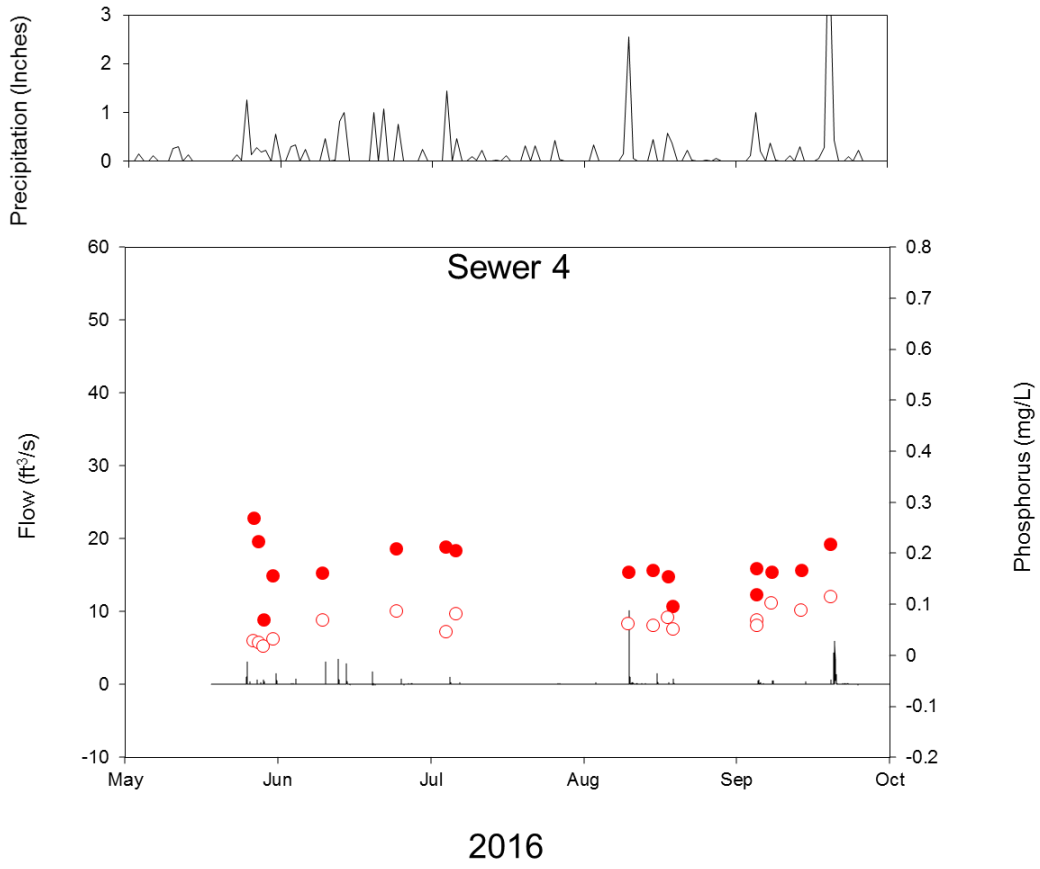

Figure31. *Variations in flow and phosphorus concentrations for storm sewer 4 in 2016*

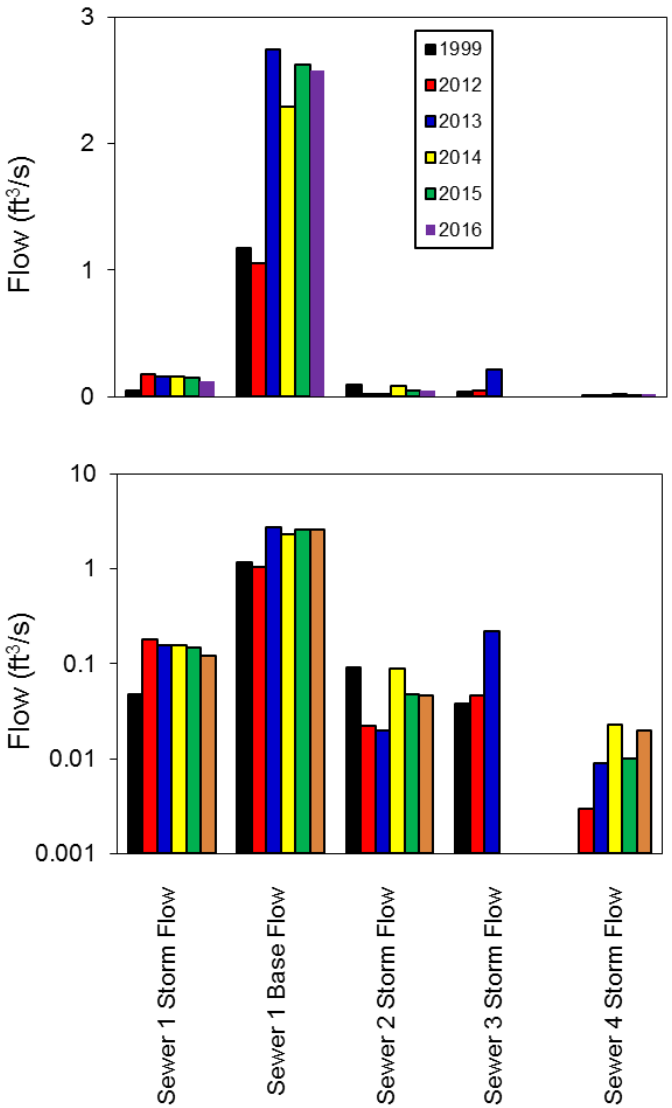

Figure 32. *Comparison of mean summer flow at various storm sewers in 1999 and 2012-16. Please note the log scale in the lower panel.*

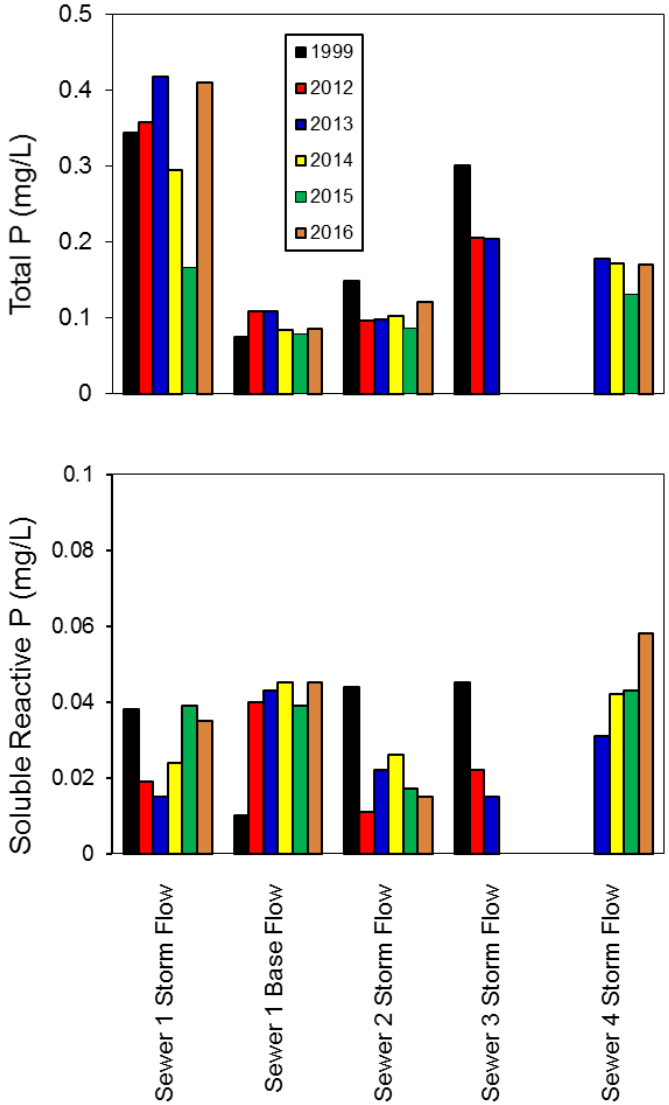

Figure 33. *Comparison of flow-weighted total and soluble reactive phosphorus (P) concentrations at various storm sewers in 1999 and 2012-16.*

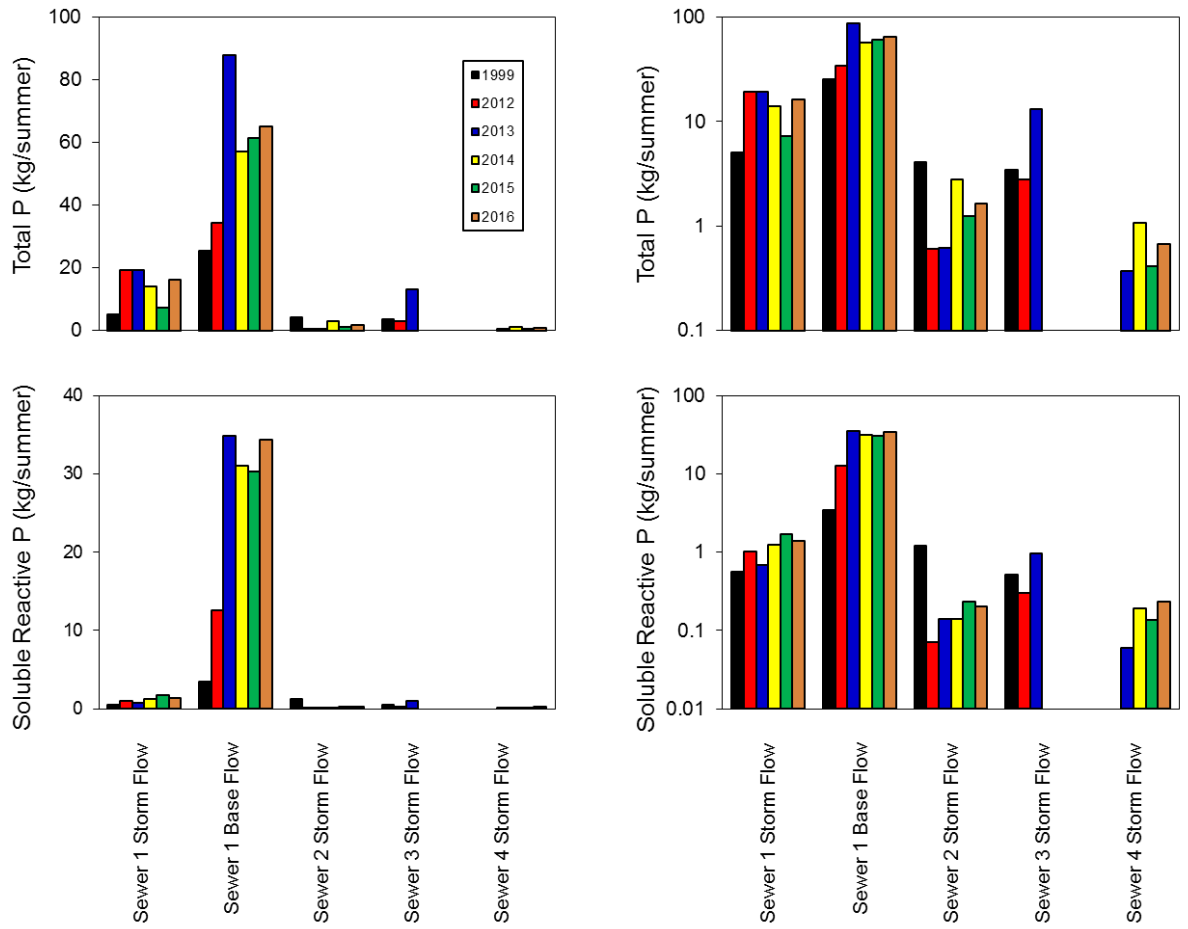

Figure 34. *Comparison of total and soluble reactive phosphorus (P) loading at various storm sewers in 1999 and 2012-16.*